(2)

223500-1-F

Final Report

AN ASSESSMENT OF THE CD-FLIR AS AN ARGUS SENSOR

D.J. WITTE

MARCH 1990

USAF Weapons Laboratory/
Advanced Radiation Office
WL/AR-G
Kirtland AFB, NM 87117-6008

REPORT DOCUMENTATION PAGE

Form Approved
OMB No. 0704-0188

1a. REPORT SECURITY CLASSIFICATION Unclassified	1b. RESTRICTIVE MARKINGS
2a. SECURITY CLASSIFICATION AUTHORITY	3. DISTRIBUTION/AVAILABILITY OF REPORT
2b. DECLASSIFICATION/DOWNGRADING SCHEDULE	
4. PERFORMING ORGANIZATION REPORT NUMBERS(S) 223500-1-F	5. MONITORING ORGANIZATION REPORT NUMBER(S)
6a. NAME OF PERFORMING ORGANIZATION ERIM — 6b. OFFICE SYMBOL *(if applicable)*	7a. NAME OF MONITORING ORGANIZATION
6c. ADDRESS (City, State, and ZIP Code) P.O. Box 8618 Ann Arbor, MI 48107	7b. ADDRESS (City, State, and ZIP Code)
8a. NAME OF FUNDING /SPONSORING ORGANIZATION USAF WL/AR-G — 8b. OFFICE SYMBOL *(if applicable)*	9. PROCUREMENT INSTRUMENT IDENTIFICATION NUMBER
8c. ADDRESS (City, State, and ZIP Code) WL/AR-G Kirtland AFB, NM 87117-6008	10. SOURCE OF FUNDING NUMBERS PROGRAM ELEMENT NO. — PROJECT NO. — TASK NO. — WORK UNIT ACCESSION NO.

11. TITLE (Include Security Classification)
An Assessment of the CD-FLIR as an ARGUS Sensor

12. PERSONAL AUTHOR(S)
David J. Witte

13a. TYPE OF REPORT	13b. TIME COVERED	14. DATE OF REPORT (Year, Month, Day)	15. PAGE COUNT
Final	FROM Jan90 TO Mar90	March 1990	57 + x

16. SUPPLEMENTARY NOTATION
The WL/AR-G Technical Monitor was Lt. Claron Jorgensen, USAF
The Principal Investigator was Mr. David Witte, ERIM

17. COSATI CODES			18. SUBJECT TERMS *(Continue on reverse if necessary and identify by block number)*
FIELD	GROUP	SUB-GROUP	Infrared, Radiometry, Calibration, Missile plumes

19. ABSTRACT *(Continue on reverse if necessary and identify by block number)*

The CD-FLIR is U.S. Government-owned thermal imaging system that has been made available for use on the ARGUS aircraft. This report presents the results of a study in which the expected performance of this sensor is defined. Recommendations are made for several simple hardware modifications that will permit optimum sensor performance. Also, the performance impact of using analog vs. digital recording is considered.

20. DISTRIBUTION/AVAILABILITY OF ABSTRACT ☒ UNCLASSIFIED/UNLIMITED ☐ SAME AS RPT. ☐ DTIC USERS	21. ABSTRACT SECURITY CLASSIFICATION Unclassified
22a. NAME OF RESPONSIBLE INDIVIDUAL	22b. TELEPHONE (Include Area Code) — 22c. OFFICE SYMBOL

EXECUTIVE SUMMARY

The Calibrated Digital FLIR (CD-FLIR) is U.S. Government-owned sensor that has been made available for use on the ARGUS aircraft. This sensor offers a combination of high spatial resolution, high radiometric sensitivity, and absolute radiometric calibration within the Long Wave InfraRed (LWIR) band. This band is not presently covered by any of the other available ARGUS sensors. This report addresses two key issues related to making the CD-FLIR a useful ARGUS sensor: (1) required instrument modifications; and (2) digital versus analog data recording.

Several electronics modifications are required in order to make the CD-FLIR a useful ARGUS sensor. These are necessary because the sensor was originally designed to operate in terrestrial scenarios with background temperatures around 300 Kelvin. The ARGUS mission environment typically involves very cold sky backgrounds having apparent temperatures of approximately 160 Kelvin. In its present configuration, the CD-FLIR can collect data against such cold backgrounds, but only with an unacceptably large penalty in radiometric sensitivity.

An analysis was performed to determine what instrument modifications will permit full-sensitivity operation against very cold backgrounds. The analysis considered measurement requirements derived from the missile plume phenomenology community, as these translate into the most stressing sensor requirements. A number of relatively simple sensor modifications are identified in Section 2.0 of this report that should permit complete measurement of predicted plume signatures down to the ultimate sensitivity limit of the CD-FLIR (which has an Noise Equivalent Spectral Radiance of 8.7E-6 Watts/(cm**2-sr-um) at its entrance aperture).

The CD-FLIR has both digital and analog data outputs. The performance characteristics that make it attractive for use on the ARGUS platform are, however, only realized with the digital output. A digital recording capability suitable for supporting ARGUS missions does not presently exist. For the near term, it appears that the analog output will have to be used, even though this implies less than full system performance.

Section 3.0 of this report describes the performance penalties associated with the CD-FLIR's analog output. Specifically, the issues of reduced radiometric sensitivity, reduced spatial resolution, and reduced calibration accuracy are addressed. Compared to the digital output, system spatial resolution is expected to degrade by at least a factor of two, while radiometric sensitivity may as much as an order of magnitude worse. Radiometric calibration of analog data appears to be feasible, however, as the expected errors appear to be tolerable.

TABLE OF CONTENTS

LIST OF FIGURES

LIST OF TABLES

1.0

INTRODUCTION

1.1 BACKGROUND

The Calibrated Digital FLIR (CD-FLIR) is a U.S. Government-owned sensor that has been made available for use on the ARGUS aircraft. This sensor offers a combination of high spatial resolution, high radiometric sensitivity, and absolute radiometric calibration within the Long Wave InfraRed (LWIR) band. This band is presently not covered by any of the other available ARGUS sensors.

The CD-FLIR was originally designed for target sensing in terrestrial environments in which the background temperature is in the range 270-320 Kelvin. Nearly all of the ARGUS missions, however, involve very cold sky backgrounds with apparent temperatures typically around 160 Kelvin. Although the CD-FLIR is able to collect useable data against such low background temperatures, its present configuration is such that a significant penalty in sensitivity is required. Specifically, the only available gain setting that presently permits low background operation is so low that the inherent system sensitivity is degraded by about a factor of four. With the Narrow Field of View (NFOV) telescope, the inherent sensitivity expressed as a Noise Equivalent Spectral Radiance (NESR) is 8.7E-7 Watts/[cm**2-sr-um]. This is only slightly better than the minimum performance specification set by SDIO (i.e., NESR no larger than 1.0E-6 Watts/(cm**2-sr-um)); thus, a four-fold degradation is generally unacceptable.

There are two other gain settings presently available on the front panel of the CD-FLIR. Both provide full system sensitivity, but are unsuitable for data collection against background temperatures lower than about 255 Kelvin. This limitation is imposed by the system dynamic range, as discussed further in Section 1.3. Thus, in its present configuration, the CD-FLIR is not capable of providing useful data in a typical ARGUS mission. In order to make it capable, hardware modifications to the instrument are necessary.

In addition to the requirement for instrument modification, a second fundamental issue exists regarding the use of the CD-FLIR as an ARGUS sensor. This concerns the type of data recording system to be used with the FLIR. The CD-FLIR has two primary signal outputs; one produces digital data with ten-bit resolution, while the other provides RS-170 standard video. The system sensitivity value quoted above applies only to the digital output data; thus, a digital recording system is required in order to realize that sensitivity. Due to the limited dynamic range of analog video signals (equivalent to seven or eight bits resolution) the effective sensitivity of the video output is worse than that of the

digital output. The amount of degradation has yet to be quantified, but is expected to be such that the minimum sensitivity required by SDIO cannot be attained with analog video data.

From a technical standpoint, it would appear that a digital recording capability is mandated; however, there are practical considerations, particularly in the short term, that may necessitate use of analog data recording. Chief among these is the absence of any existing digital recording system that is both compatible with (i.e., can interface directly with) the CD-FLIR and is able to record 30 frames per second (another SDIO requirement). The existing digital recorder for the CD-FLIR is limited to four frames per second. In addition, the availability of the existing recorder may be less than adequate for supporting the ARGUS mission schedule. Thus, analog recording may be a necessary compromise until such time as a suitable digital capability becomes available.

Due to the above issues, there is some uncertainty regarding the expected level of performance of the CD-FLIR in the ARGUS environment. As a result, ERIM conducted a study of these issues, the results of which are presented in this report. The specific study objectives are summarized in Section 1.2. Section 1.3 follows with a brief description of the CD-FLIR's operation. Section 2.0 then presents an analysis in which the hardware modifications required for full sensitivity against cold backgrounds are identified and evaluated in terms of their effects upon sensor performance. Section 3.0 examines the impact of processing analog video data upon sensor performance and calibration accuracy. Section 4.0 presents a summary and conclusions.

1.2 STUDY OBJECTIVES

Three specific objectives were defined to assess the CD-FLIR's expected performance in the ARGUS environment:

1. Identify the hardware modifications necessary to permit data collection against very cold backgrounds with maximum radiometric sensitivity.

2. Assess the impact of processing data from the CD-FLIR's video output upon system performance and radiometric calibration accuracy.

3. Define the expected level of performance of the CD-FLIR in terms of its ability to measure missile plumes.

The motivation behind the first two objectives was explained in the previous section. Objective #3 was defined for two reasons. The measurement of missile plume characteristics is perhaps the most important, as well as the most demanding, ARGUS mission for which the CD-FLIR will be used. Thus, defining the FLIR's performance for this application provides a clear assessment of its utility as an ARGUS asset.

The second reason for defining Objective #3 was simply to identify a set of sensor performance requirements for use in conjunction with Objectives #1 and #2. Three predicted plume signatures were obtained from Dr. William Jeffery of the Institute for Defense Analysis (IDA). The signatures were calculated using the CHARM computer code. Two-dimensional plots of iso-radiance contours in the 8.0-12.0 micrometer band were provided for three signature strengths: weak, intermediate, and strong. These data were used to define the performance requirements of the CD-FLIR in terms of sensitivity, dynamic range, field of view, and spatial resolution.

1.3 REVIEW OF SENSOR OPERATION

In order to discuss both the hardware modifications and the ramifications of processing video data, a review of the CD-FLIR's operational characteristics is appropriate. For the purposes of this report, the relevant aspects of the FLIR's operation are represented by the following three topics:

1. The optical path between the target and the CD-FLIR's internal reference plane (i.e., the location of the internal calibration sources).

2. The signal processing electronics between the detectors and the analog-to-digital (A/D) converters.

3. The methodology used to create analog video imagery from the digital frame buffer.

Each of these topics is discussed below.

1.3.1 Radiance Propagation Path

Figure 1 is a schematic representation of the optical path between a target and the FLIR focal plane. The target of interest, a missile plume, is assumed to have an angular size greater than the FLIR instantaneous field of view (IFOV). Thus, the radiant output of the plume may properly be expressed in units of radiance. As shown in Figure 1, the inherent, or zero-range, target radiance propagates through some atmospheric path that both attenuates the target energy and contributes radiance of its own. A portion of the resulting radiance field incident upon the ARGUS aircraft window is then transmitted by the window to the entrance aperture of the FLIR telescope. The window also contributes thermal energy that is a combination of: (1) window self-emission; and (2) reflection of the internal aircraft environment in the immediate vicinity of the sensor. Similarly, the telescope transmits some fraction of its received energy and also emits and reflects additional energy.

The total radiance level at the reference plane is given by Equation 1, shown in Figure 2. The contributions of the target, atmosphere, aircraft window, and FLIR telescope are shown

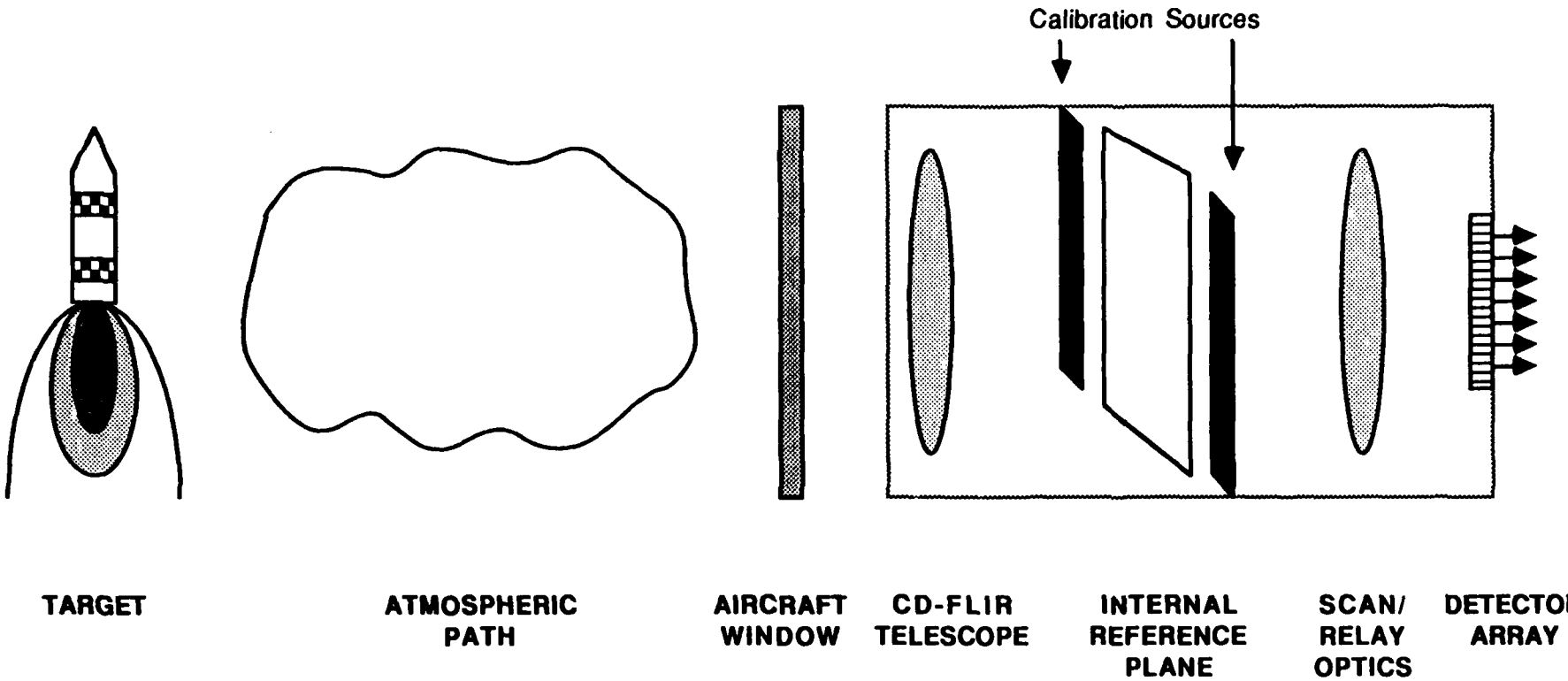

Figure 1. Radiance Propagation Path

explicitly in Equation 1. Because the reference plane is the location of the FLIR's internal calibration sources, the radiometric effects of the scan/relay optics between the reference plane and detectors may be ignored. This point is explained further in Section 1.3.2.

The internal reference plane is an itermediate image plane that is re-imaged and scanned onto a 160-element detector array by the scan/relay optics. A horizontal bidirectional scan is used in conjunction with the vertically-oriented detector array to create a two-dimensional image. Individual detector elements are separated from one another by approximately one line width.

From the standpoint of the reference plane, the image of the detector array is swept first from the right side to the left side in 1/60th of a second, then drops vertically by one line width and scans from left-to-right in another 1/60th second. The two resulting 160-line images are interlaced to form a 320 line frame every 1/30th second. Each line is sampled to produce 1024 horizontal pixels over the active field of view, which includes the two adjustable-temperature calibration reference sources. There are two additional radiance sources at the reference plane that are located just outside the active field of view. These sources, illustrated in Figure 3, are herein referred to as the "dc restoration references." Their purpose is discussed in Section 1.3.2. It should be noted, as is indicated in Figure 3, that the temperatures of the dc restoration references are slaved to that of the left calibration reference.

1.3.2 Signal Processing Electronics

Figure 4 illustrates the electronics chain used to amplify and digitize the signal out of a given detector element. Each of the 160 detector channels has its own associated electronics. As shown in Figure 4, radiant flux incident upon the detector produces an output voltage that is capacitively coupled (i.e., ac coupled) into the pre-amplifier denoted by "G1." The pre-amp output is ac coupled into a post-amplifier, denoted by "G2." The post-amp output is ac coupled into the A/D module, where a final buffer amplifier "G3," (which has a gain near unity) produces voltages that are then converted into ten-bit digital values.

In order to facilitate radiometry, the detector signals are clamped to a dc voltage reference that is applied just before the G3 amplifier, as shown in Figure 4. Specfically, during the turn-around time of the horizontal scan mirror--that is, just before the active FOV (including the calibration sources) is scanned--the detectors view one of the dc restoration radiance references (cf., Figure 3). During this period, the clamp voltage switch shown in Figure 4 is closed and the coupling capacitor between G2 and G3 quickly charges up to the clamp voltage (nominally, 3.4 volts). As the detector (image) approaches the adjacent calibration source, the clamp switch is opened. The change in flux at the detector due to viewing the calibration source produces a signal change that propagates normally through the electronics chain. As an example,

EQUATION 1:

$$L_{rp} = \tau_{tel}\,\tau_{win}\,\tau_{atm}\,L_{plm}$$ Target component

$$+ \tau_{tel}\,\tau_{win}\,L_{atm}$$ Atmosphere component

$$+ \tau_{tel}\left[\,\varepsilon_{win}L_{BB}(T_{win}) + \rho_{win}L_{BB}(T_{amb})\,\right]$$ Window component

$$+ (1 - \tau_{tel})\,L_{BB}(T_{tel})$$ Telescope component

SYMBOL DEFINITIONS:

L_{rp} = Total in-band radiance level at the CD-FLIR internal reference plane

L_{plm} , L_{atm} = In-band radiances of the Plume and Atmospheric Path, respectively

$\tau_{atm}, \tau_{win}, \tau_{tel}$ = Transmissivities of the Atmosphere, A/C Window, and Telescope, respectively

$\varepsilon_{win}, \rho_{win}$ = Aircraft window Emissivity and Reflectivity, respectively

$L_{BB}(T)$ = In-band radiance from a BlackBody at temperature "T"

$T_{win}, T_{amb}, T_{tel}$ = Temperatures of the A/C Window, Interior Ambient, and Telescope, respectively

Figure 2. Equation 1: Components of Total Reference Plane Radiance

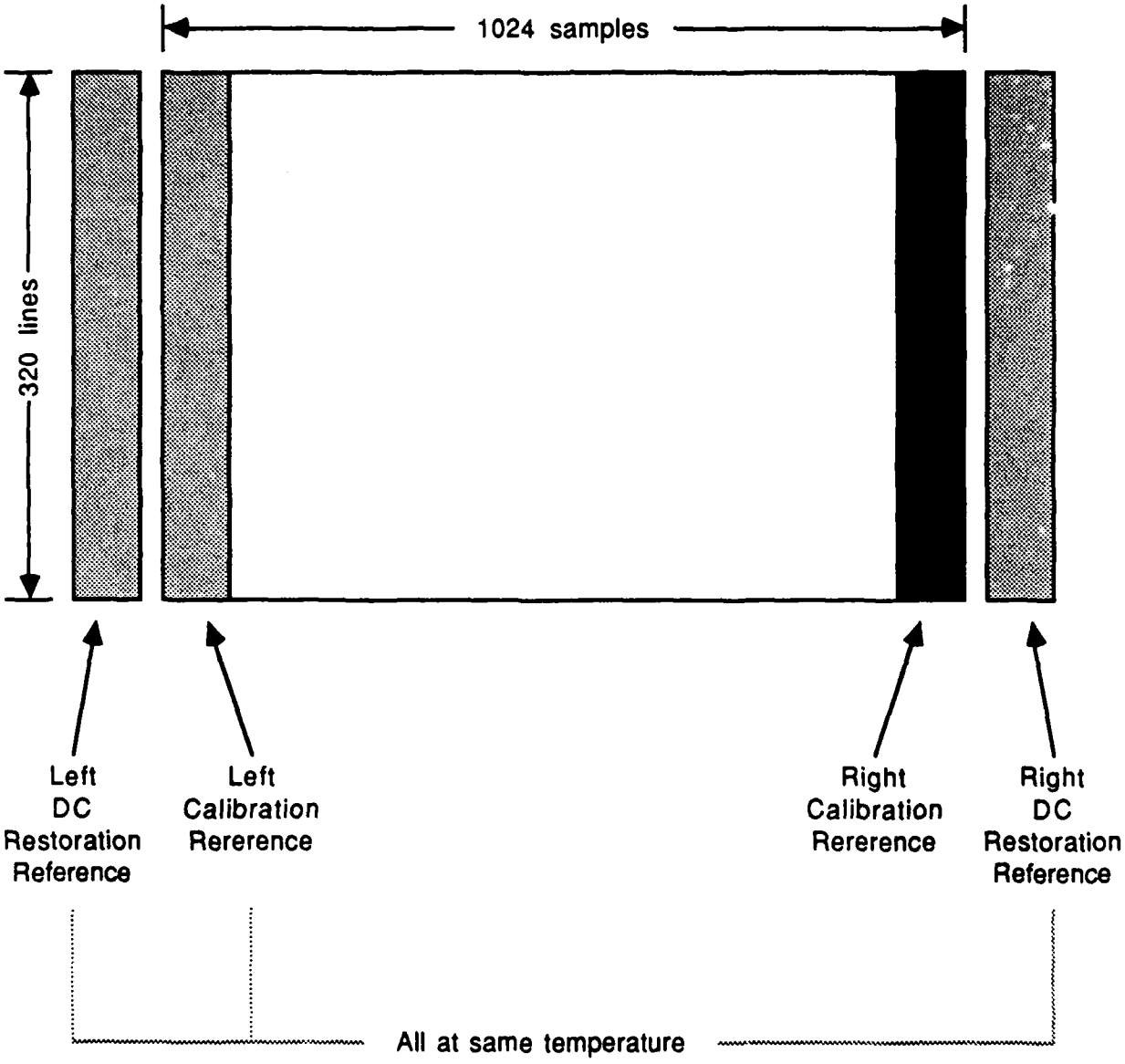

Figure 3. CD-FLIR Reference Plane Source Configuration

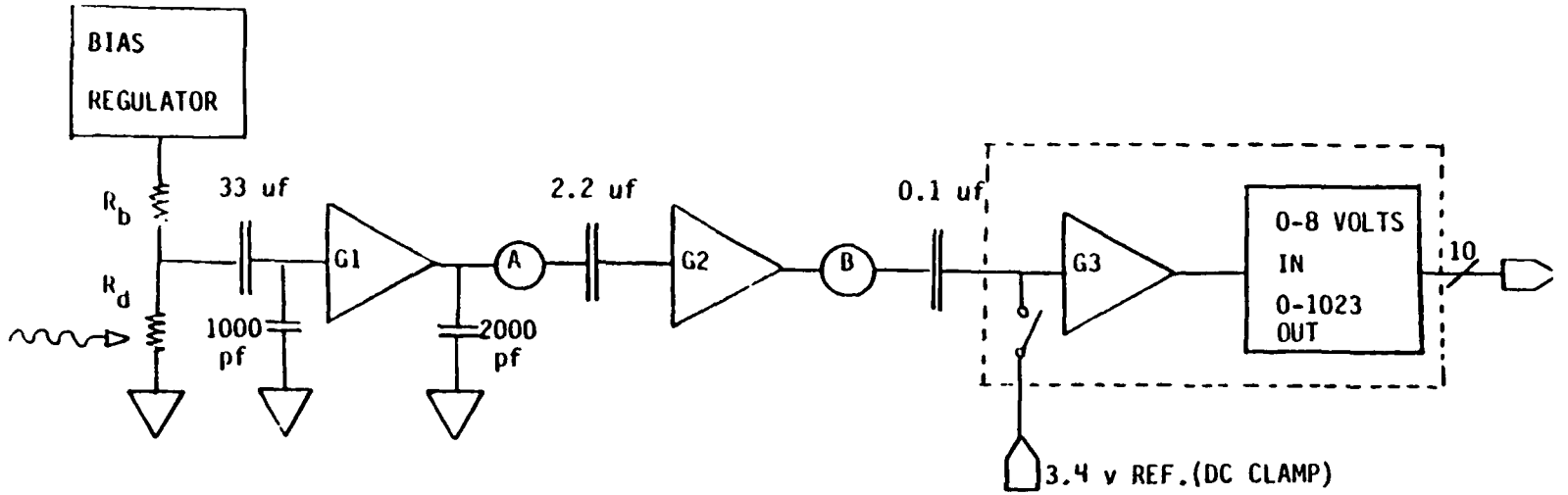

8

G1
70 MIN
75 NOM
80 MAX

G2

	MIN		NOM		MAX		
1	- 0	1:	0	0:	0	1:	V/V
2	15	2:	16	0:	16	8:	V/V
3	19	8:	20	8:	21	8:	V/V
4	25	8:	27	2:	28	6:	V/V
5	33	4:	35	2:	37	0:	V/V
6	41	0:	43	2:	45	4:	V/V
7	48	6:	51	2:	53	8:	V/V
8	54	7:	57	6:	60	5:	V/V
9	60	8:	64	0:	67	2:	V/V
10	66	9:	70	4:	73	9:	V/V
11	77	5:	81	6:	85	7:	V/V
12	91	2:	96	0:	100	8:	V/V
13	109	4:	115	2:	121	0:	V/V
14	139	8:	147	2:	154	6:	V/V
15	182	4:	192	0:	201	6:	V/V
16	243	2:	256	0:	268	6:	V/V

G3
1-4 MIN
1-5 NOM
1-6 MAX

Attenuation of 0.8-1.0 also available

(A)
RANGE = +/- 0.5 V
DET NOISE = 28-280 μV

(B)
RANGE = +/- 5.0 V
DET NOISE = 1.8-17 mV

Figure 4. CD-FLIR Detector Electronics

assume this signal change has a magnitude of one volt after the second amplifier stage (i.e., at point "B" in Figure 4). At the input to the A/D converter, this signal will have a dc level of 4.4 volts because of the 3.4 volt increase it obtains from passing through the final coupling capacitor (recall that stage G3 has effectively unity gain).

The point of the above example is to illustrate how the ac coupled signals passing through the electronics chain represent flux differences relative to the radiance level of the dc restoration sources. These differences are then biased with a dc level (i.e., the dc level is "restored"), which is maintained across the third coupling capacitor, before they are digitized to ten bits. Several observations may be made regarding this scheme:

1. As shown in Figure 4, the 0 - 8 volt input range of the A/D converter is linearly mapped into 0 - 1023 digital counts.

2. If the detector views a flux level equal to that of the dc restoration source, the zero flux difference produces a zero signal difference. The resulting voltage at the A/D input is 3.4 volts, which produces a digital level of approximately 435. Ideally, this is the situation that should hold with the left calibration reference, as its temperature and those of the dc restoration sources are supposed to be identical. Note that output digital values are related to radiance differences at the FLIR's internal reference plane. The effects of the scan/relay optics (cf., Figure 1) cancel out in the differencing operation.

3. Referenced to the A/D input, signals in the range 0 - 3.4 volts (digital levels 0 - 435) represents flux levels less than that of the dc restoration source(s), while the range 3.4 - 8.0 volts (435 - 1023) represents higher flux levels.

4. If a scene element produces a flux level that differs too greatly from that of the dc restoration sources, the resulting signal will lie outside the 0 - 8 volt range and so will not be measurable. This occurs for very cold as well as very hot scene features.

5. The range of absolute target radiance levels that is measureable (i.e., produces signals within the 0 - 1023 digital count range) depends upon: (a) the dc restoration source temperature (and, therefore, the left calibration source temperature); (b) the total gain of the detector/electronics chain; and (c) the effects of any intervening media between the target and the FLIR reference plane. Equation 1 (cf., Figure 1) accounts for this last consideration. The first two are represented in Equation 2, which is shown in Figure 5.

6. Given dc restoration source radiance and total system responsivity, Equations 1 and 2 may be used to quantify the range of target radiances measurable with the FLIR.

EQUATION 2:

$$D_T = RRP(g)\left[L_{rp} - L_{clamp} \right] + D_{clamp}, \quad 0 < D_T < 1023$$

SYMBOL DEFINITIONS:

D_T = Target Digital Value output by the FLIR

L_{rp} = Radiance at the Reference Plane (related to target radiance via Eq. 1)

L_{clamp} = Radiance of the DC Restoration Source

$RRP(g)$ = Responsivity [digital counts/unit radiance] at the Reference Plane @ Gain "g"

D_{clamp} = *Digital value corresponding to the DC Restoration bias voltage*

Figure 5. Equation 2: Digital Output vs. Reference Plane Radiance

There are several other aspects of the detector electronics that are relevant to this study. One is "low-frequency droop," or simply "droop." Droop is the tendency for low-frequency signals (e.g., those from large, uniform scene features) to migrate over time toward a fixed reference level. In the case of the CD-FLIR, the reference level is the 3.4 volt clamp level, which corresponds to digital level 435. Physically, droop results from the finite RC time constant associated with the coupling capacitors--especially the third capacitor--shown in Figure 4. As mentioned above, when the clamp voltage switch is thrown, the third capacitor quickly charges toward the 3.4 volt level. The quick charging occurs because the capacitor is connected with a relatively small resistance. When the clamp switch is opened, the capacitor is connected to the comparatively large input impedance of the G3 amplifier. The resulting RC time constant is not large enough to ignore, however, as it is approximately 33 milliseconds. For comparison, the field of view is scanned once in roughly 12.5 milliseconds, or about one third of a droop time constant.

With the clamp switch open, the coupling capacitor tries to charge (or discharge) to the average level of whatever signals are passing through it, which is equivalent to saying that it attempts to block the signal's dc level. Given enough time (e.g., four to five time constants), it would achieve this goal. The resulting dc level of the output signal would then be the 3.4 volt "initial condition" that was applied to the capacitor during the clamping process. By resetting the capacitor voltage prior to each scan of the active FOV, this tendency is minimized, but not entirely avoided. During the 12.5 msec scan, the capacitor voltage partially charges toward the average level of the signals passing through it. The result is droop.

The significance of droop is that uniform input scenes appear as non-uniform images, which are therefore radiometrically in error. As a specific example relevant to the present study, consider the FLIR viewing a cold sky background. Assume the gain and clamp reference level are such that the resulting digital level of the sky should be 35 counts, i.e., 400 counts below the clamp level of 435. The detectors view the cold sky for roughtly 11 msec each scan (the remain 1.5 msec are spent viewing the calibration sources). During the 11 msec, the sky signal will droop in decaying exponential fashion toward digital level 435. For a 33 msec droop time constant, the amount of droop at the end of the scan will approximately be given by

$$\text{Droop after 11 msec} = (400 \text{ counts}) * [1 - \exp(-11 \text{ msec}/33 \text{ msec})]$$

$$= 113 \text{ counts}$$

Thus, by the end of the scan, the digital value of the sky background will be 35 + 113 = 148. The corresponding relative radiometric error (defined in terms of the radiance difference between the sky and the dc restoration source) is 113/400 * 100% = 28 percent. The amount of absolute radiometric error depends upon the absolute sky radiance and the radiance difference corresponding

to 113 digital counts.

The above example is illustrated qualitatively in Figure 6. Note the dependence upon scan direction of the resulting droop patterns. ERIM has developed a droop-correction algorithm for use on CD-FLIR digital data that removes droop-induced signal errors, on a line-by-line basis, for any arbitrary input scene.

The remaining aspects of the CD-FLIR electronics pertinent to the present study are that: (1) there are 15 global gain levels available for selection; and (2) in addition, each of the 160 detector channels has its own programmable gain and offset.

Referring to the lower portion of Figure 4, the minimum, nominal, and maximum gain values for the three amplifier stages are listed. A table is shown for stage G2, which is known as the Variable Gain Variable Frequency Filter (VGVFF), listing sixteen discrete gain settings numbered 1 through 16. Setting '1' produces zero gain, and so is of no practical value. The remaining 15 settings represent a wide range of total system responsivities that are potentially available. At present, the LOW, NOMINAL, and HIGH gain settings that are selectable on the CD-FLIR control panel correspond to VGVFF gain settings 2, 13, and 16, respectively. One of the key elements of the present study is to consider the value of utilizing other VGVFF gain settings.

As mentioned above, each of the 160 detector electronics chains has its own associated gain and offset. This feature is used to equalize the response characteristics of the individual detector elements for the purpose of reducing channel-to-channel pattern noise. This function is implemented in the A/D module. Each channel has a gain and offset coefficient stored in firmware that is used to correct the analog detector signal just prior to digitization.

The significance of the on-board detector normalization is that a unique set of coefficients must be applied for any VGVFF gain that is selected. There is only room, however, to store coefficients for two gain levels. At present, the NOMINAL and HIGH gain settings are normalized, while the LOW setting is not. If, as will be recommended later in this report, new VGVFF settings are chosen, it will be necessary to have the FLIR manufacturer (Texas Instruments) define new normalization coefficients to replace those currently stored in the sensor firmware.

1.3.3 Creation of Analog Video Output

The final topic concerning the CD-FLIR's operation concerns the method by which RS-170 standard video output is created from the pixel values of the digital output data stream. The 30 Hz frame rate of the CD-FLIR is inherently compatible with the RS-170 standard; however, the 320 by 1024 digital frame dimensions are not. Under the RS-170 standard, a 525-line TV frame having 480 active lines (the remainder represents the vertical blanking period) is created by a 2:1 interlace of two 252.5 line fields

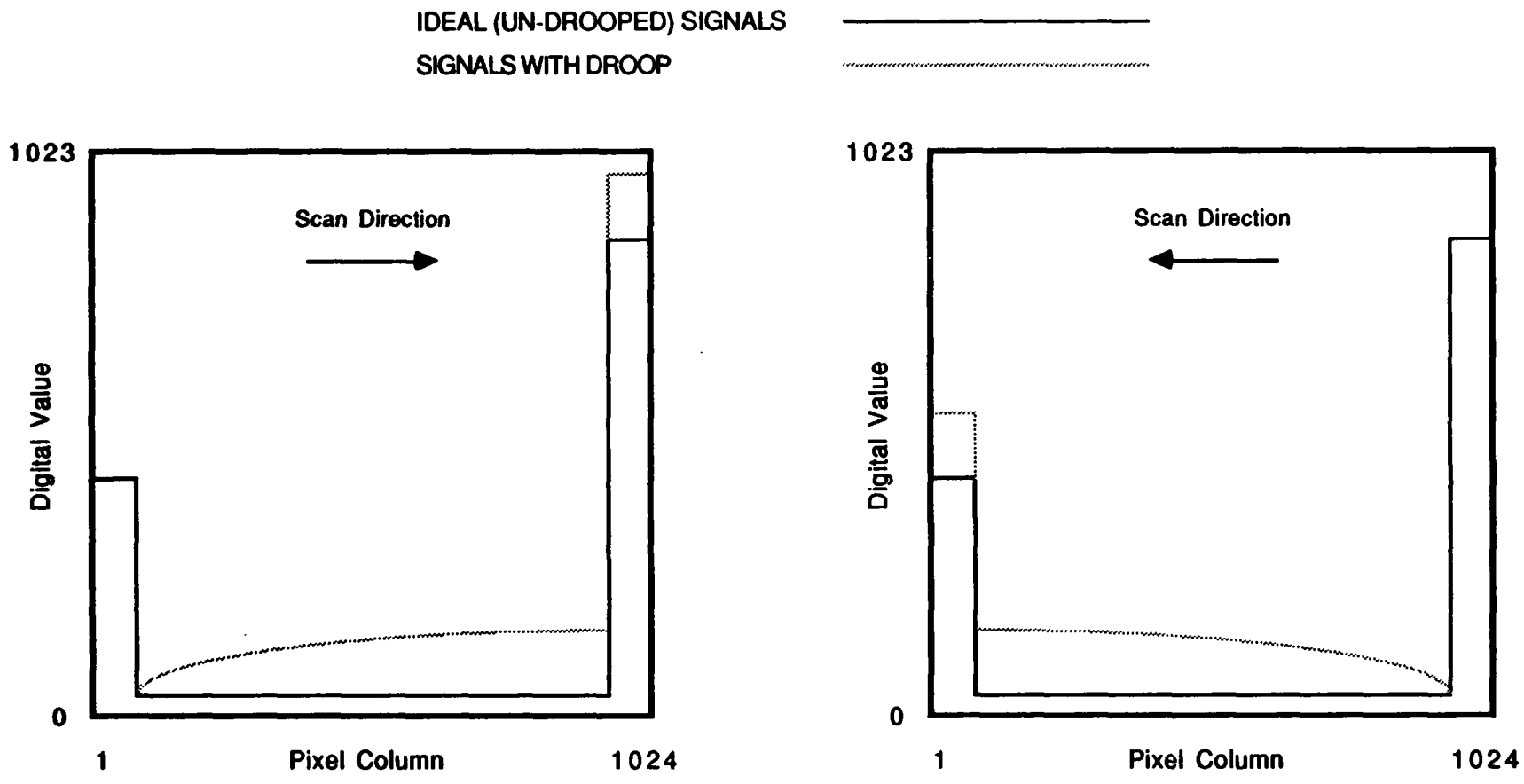

Figure 6. Illustration of Signal Droop for a Cold Uniform Scene

(each having 240 active lines). Each of the fields is painted out in 1/60th of a second.

In the CD-FLIR, each 320 line digital frame is used to create a single video field that is painted out twice (i.e., interlaced with itself) in 1/30th second. Averaging is used to create 240 active field lines from the 320 digital frame lines. The specific averaging scheme used is illustrated in Figure 7.

As shown in Figure 7, sets of four digital lines are averaged together to produce sets of three video field lines. This achieves a 3/4 reduction, and produces exactly 240 lines from the original 320. The following comments may be made about this scheme:

1. In the digital frame, all the odd lines (line 1 is the first line at the image top) are produced by one scan direction, and all of the even lines are produced by the other. Thus, every line in the 240 line video field is the average of two lines generated by opposite scans.

2. Because droop always occurs in the direction of scan (cf., Figure 6), every video field line is an average of signals drooping in opposite directions. As a result, the existing droop-correction algorithm cannot be used on analog data.

3. Digital lines 1 and 2 are generated by Detector #1, lines 3 and 4 by Detector #2, etc. Thus, analog lines 1 and 3 are the average of two lines from a single detector; however, analog line 2 is the average of lines from two different detectors. This pattern repeats down the length of the image.

4. The 1024 horizontal samples per line in the digital data are equivalent, in terms of RS-170 signals, to a 20 MHz sample rate, or a 10 MHz bandwidth. Standard video bandwidths are roughly 4 MHz; thus, a substantial loss of horizontal resolution is to be expected in going from the digital to the analog format.

5. The line averaging degrades the vertical resolution by a factor of two. Moreover, the repeating pattern of creating three lines from four produces a spatially-varying resolution characteristic. This effect is illustrated in Figure 8 for several square-wave patterns having periods of four and eight digital lines. Depending on the phasing on the patterns relative to the digital lines, various analog patterns are produced for each frequency.

Section 3.0 presents a more detailed discussion of the ramifications of using the CD-FLIR's analog video output.

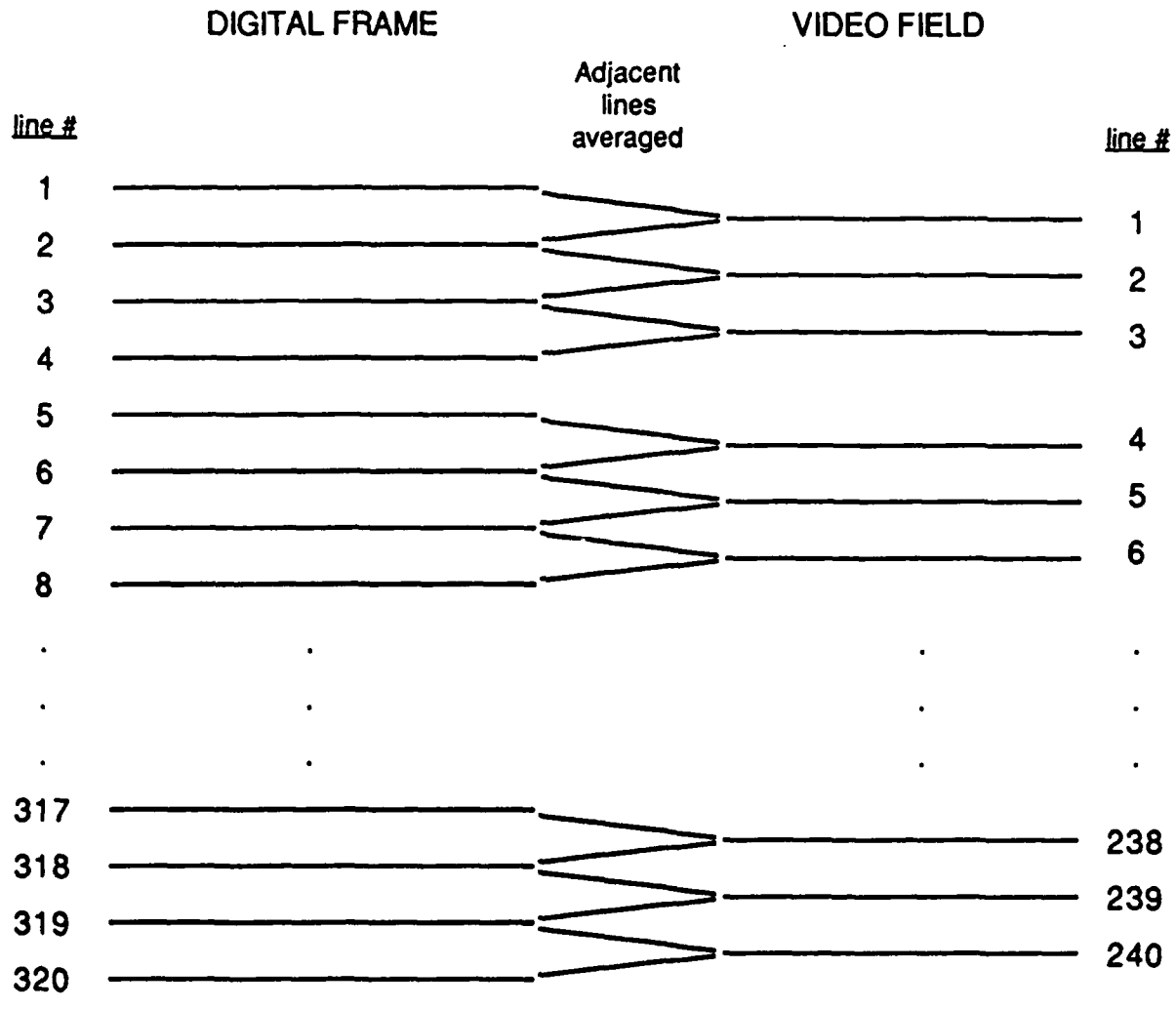

Figure 7. Creation of 240-Line Video Field from 320-Line Digital Frame

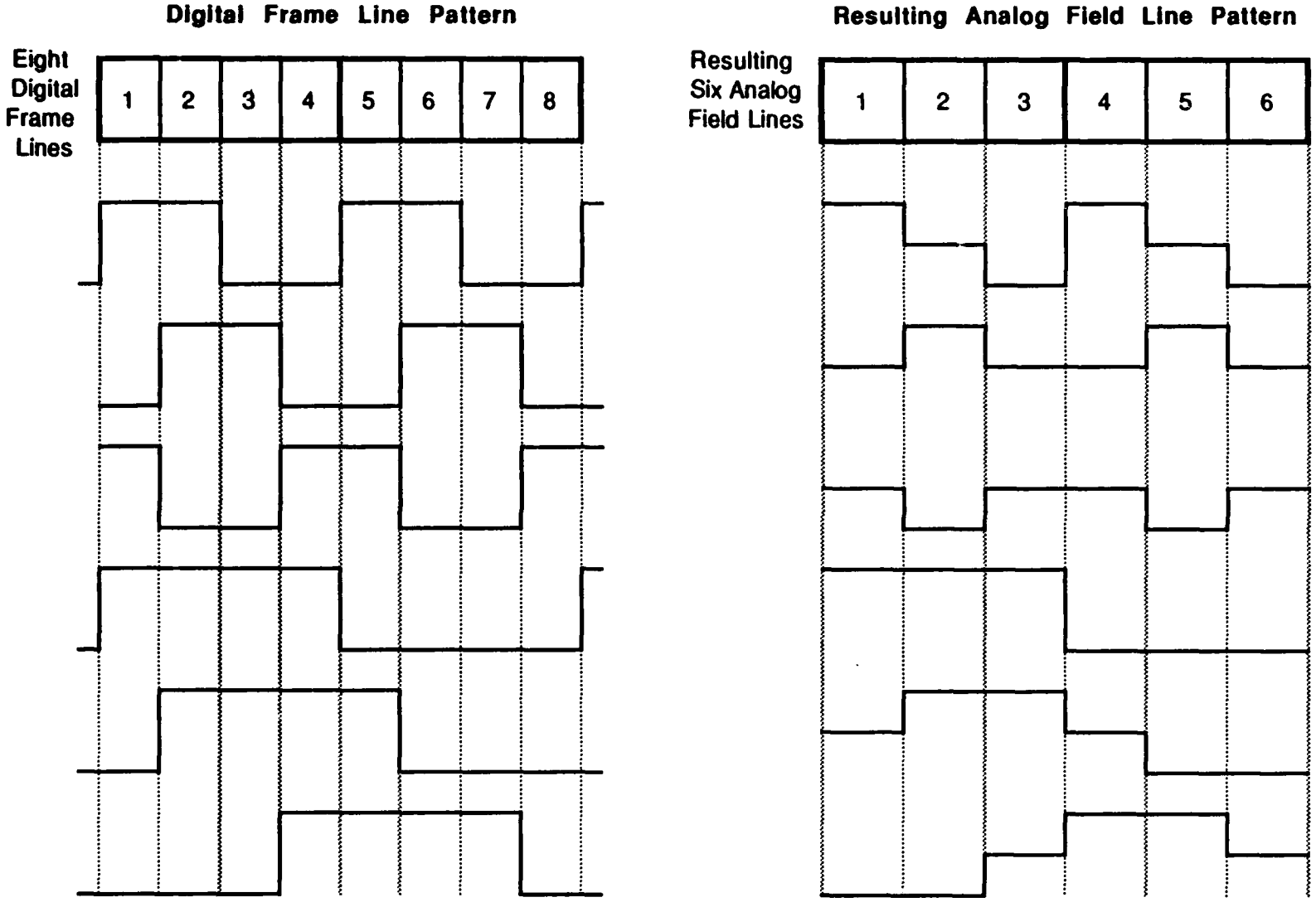

Figure 8. Spatially-Varying Frequency Response in Analog Video Output

2.0

CD-FLIR PERFORMANCE: ANALYSIS AND RECOMMENDATIONS

This section presents an analysis of the CD-FLIR's performance versus the fifteen available VGVFF gain settings that were discussed in Section 1.3.2. The purpose of this analysis is to identify which gain settings provide optimum performance in terms of radiometric sensitivity and dynamic range, while also permitting measurement against very cold sky backgrounds.

Three predicted plume signatures representing weak, intermediate, and strong signature cases, respectively, were used to define sensor performance requirements. The specific radiometric quantities used to relate these signatures--which are specified in terms of average spectral radiance across the 8.0-12.0 micrometer band--to the CD-FLIR are defined in Section 2.1. The resulting sensor performance requirements, in terms of sensitivity, dynamic range, minimum background radiance, and so forth, appear in Section 2.2. Predicted sensor performance for each VGVFF gain setting is defined and compared to these requirements in Section 2.3. Section 2.4 examines the performance benefits of changing the dc restoration bias voltage (which is presently 3.4 volts) in conjunction with selecting different VGVFF gain settings. Finally, Section 2.5 summarizes the electronics modifications that are recommended for achieving optimum performance during ARGUS missions.

2.1 DEFINITION OF RADIOMETRIC QUANTITIES

Figures 9 through 11 show the predicted plume signatures that were used to define sensor performance requirements. The signatures were provided by Dr. William Jeffrey of IDA. The format of the predictions is a two-dimensional plot of iso-spectral-radiance contours. The contours are labeled in terms of the base ten logarithm of the absolute spectral radiance; for example, -6.0 corresponds to a spectral radiance of 1.E-06 Watts/(cm**2-sr-um). Figure 9 represents a weak emission case, which results from the lack of any particulate matter in the plume. Figures 10 and 11 show, respectively, intermediate and strong emission cases. In both of these, significant amounts of particulates are present. Additional information about the plume predictions may be found in the Appendix.

The plume signature values include the effects of atmospheric attenuation along a path to an aircraft at 12 km altitude and at the slant range indicated on the plots. Atmospheric self-emission, however, has not been included, nor have the effects of the aircraft window and sensor optics. In order to predict the output of the CD-FLIR while viewing one of these plumes, it is first necessary to convert the predicted spectral radiance values into broadband radiance values at the CD-FLIR internal reference plane. In other words, it is necessary to use Equation 1 (cf., Figure 2)

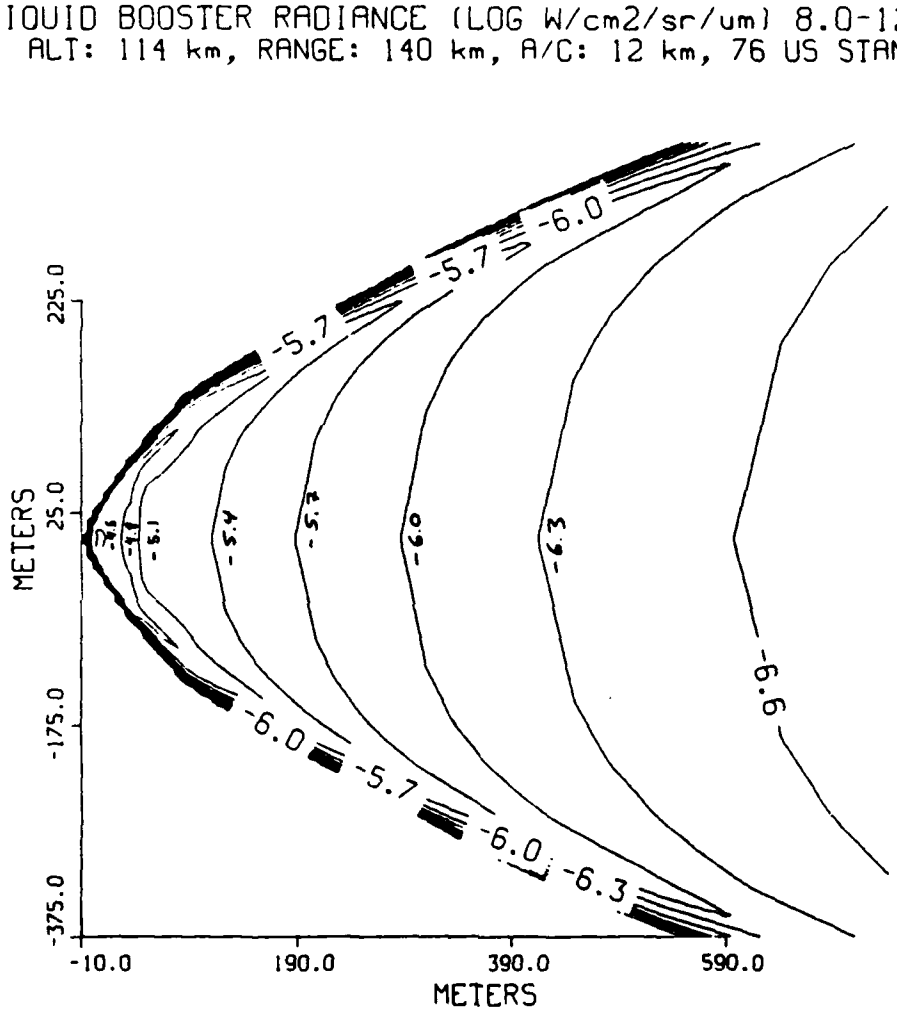

Figure 9. Predicted Plume Signature - Weak Emission Case

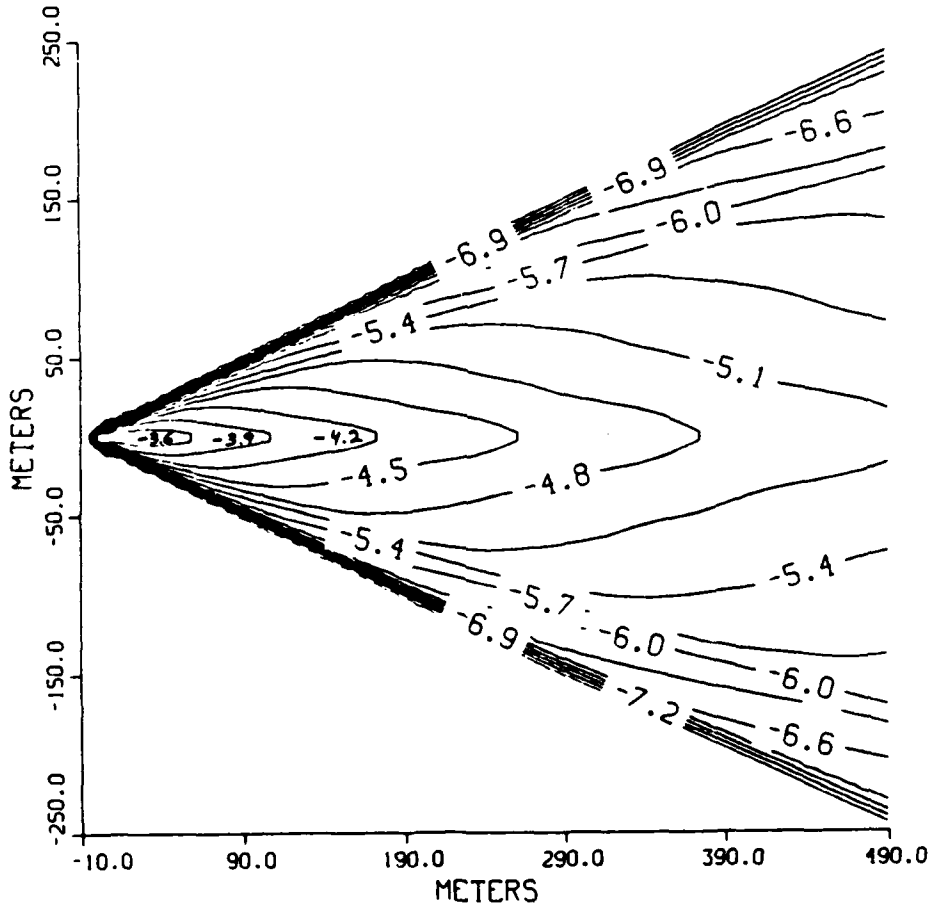

Figure 10. Predicted Plume Signature - Intermediate Emission Case

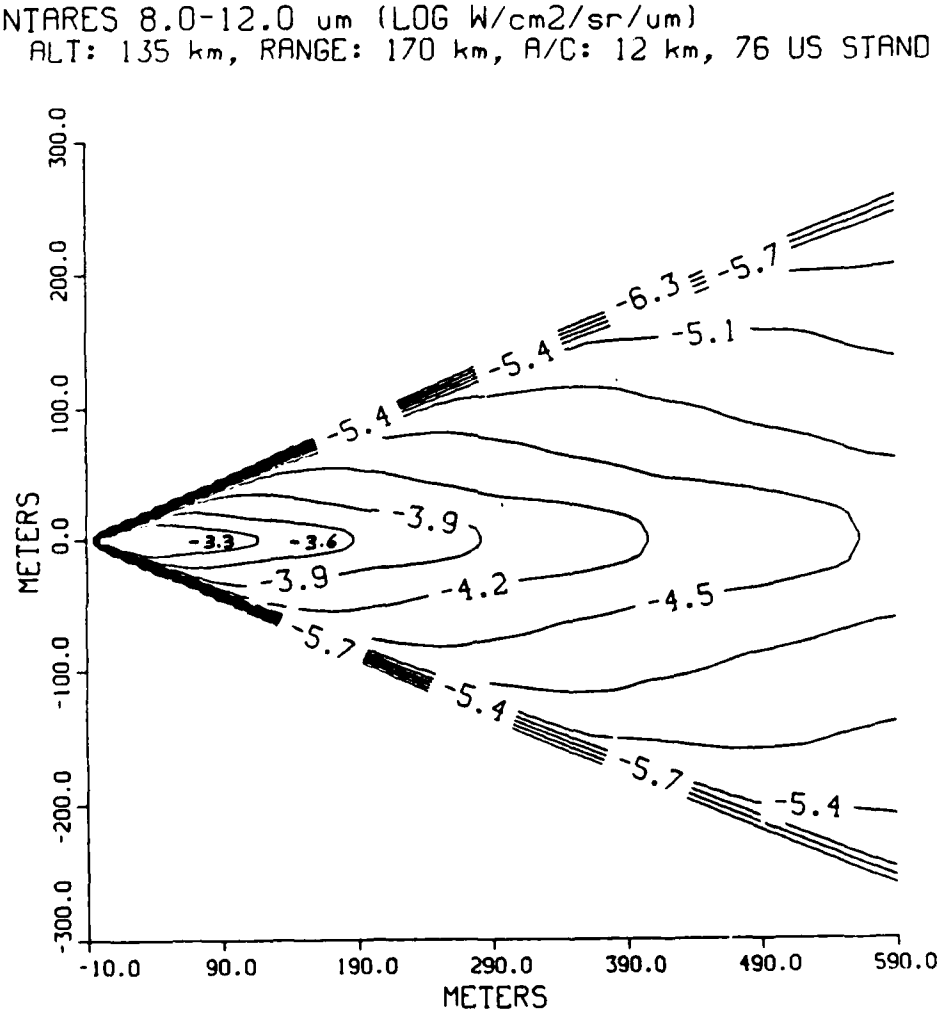

Figure 11. Predicted Plume Signature - Strong Emission Case

to predict the total radiance field received at the reference plane while viewing the plume. Once this is done, Equation 2 (Figure 5) may be used to calulate the resulting output signal for a specified gain and dc restoration reference radiance.

All of the quantities appearing in Equation 1 are defined to be in-band quantities, that is, effective quantities over the spectral bandpass of the CD-FLIR. In-band values are computed by integrating spectrally-defined values with the FLIR's relative spectral response function. This concept is illustrated in Figure 12, which shows the relative spectral response function and the results of integrating it with the Planck blackbody radiance function over a series of temperatures. The result shown represents a look-up table of in-band radiance versus blackbody temperature. This table, in conjuction with the appropriate emissivity and/or reflectivity values, is used to define the radiances of the aircraft window, the FLIR's internal reference sources, and its telescope based on their respective temperatures.

In order to convert the spectral radiance values of the plume predictions into equivalent in-band quantities, the former were multiplied by the effective spectral bandpass of the CD-FLIR. This quantity, which is simply the integral of the relative spectral response function, has a value of 3.75 micrometers. This approach ignores any spectral structure the plume signature may exhibit over the FLIR passband, but should be reasonably accurate (i.e., within ten percent error) as long as the plume has an approximately blackbody-like spectral distribution. This condition should hold for at least those cases involving particulate emissions.

The LOWTRAN6 atmospheric computer code was used to calculate the path radiance that would be received along with the plume emissions. This required computing the view geometry corresponding to each plume case. These calculations were based on the assumed 12 km aircraft altitude along with the slant range and plume altitude values shown in Figures 9 through 11.

The quantities in Equation 1 that remain to be specified are the FLIR telescope tranmissivity and the emissivity, reflectivity, and transmissivity of the aircraft window. The telescope transmissivity has been measured in the laboratory, and has a value of approximately 0.80. The transmissivity of the aircraft window was calculated from measured spectral transmission values. Actually, transmission values from two candidate windows, a germanium and a zinc sulfide window, were obtained and integrated over the CD-FLIR spectral bandpass. The spectral transmission values of the two windows over the FLIR bandpass are shown in Figure 13. The effective in-band transmissions of the two windows were calculated for a range of blackbody temperatures, as the in-band transmissivity depends on the spectral character of the energy being transmitted.

The results of the in-band window transmissivity calculations appear in Table 1. As shown, the germanium window has roughly three to five percent higher transmission than the zinc sulfide

Band Radiance Equation

$$\bar{L}(T) = \int r(\lambda)\, L_{BB}(\lambda, T)\, d\lambda$$

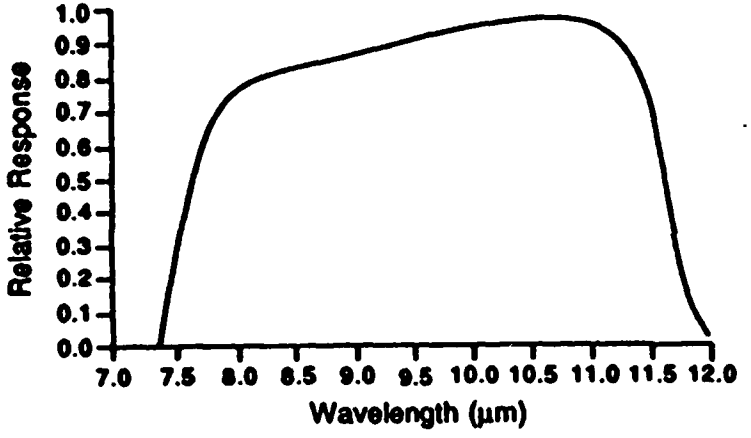

CD-FLIR Relative Spectral Response

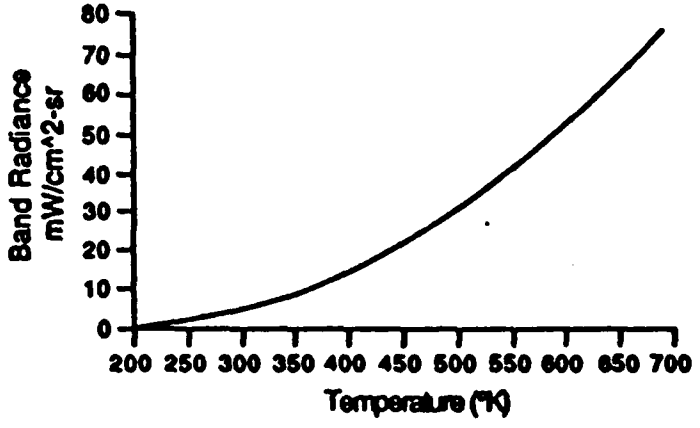

Band Radiance vs. Temperature

Figure 12. CD-FLIR Relative Spectral Response and Band Radiance vs. Temperature Functions

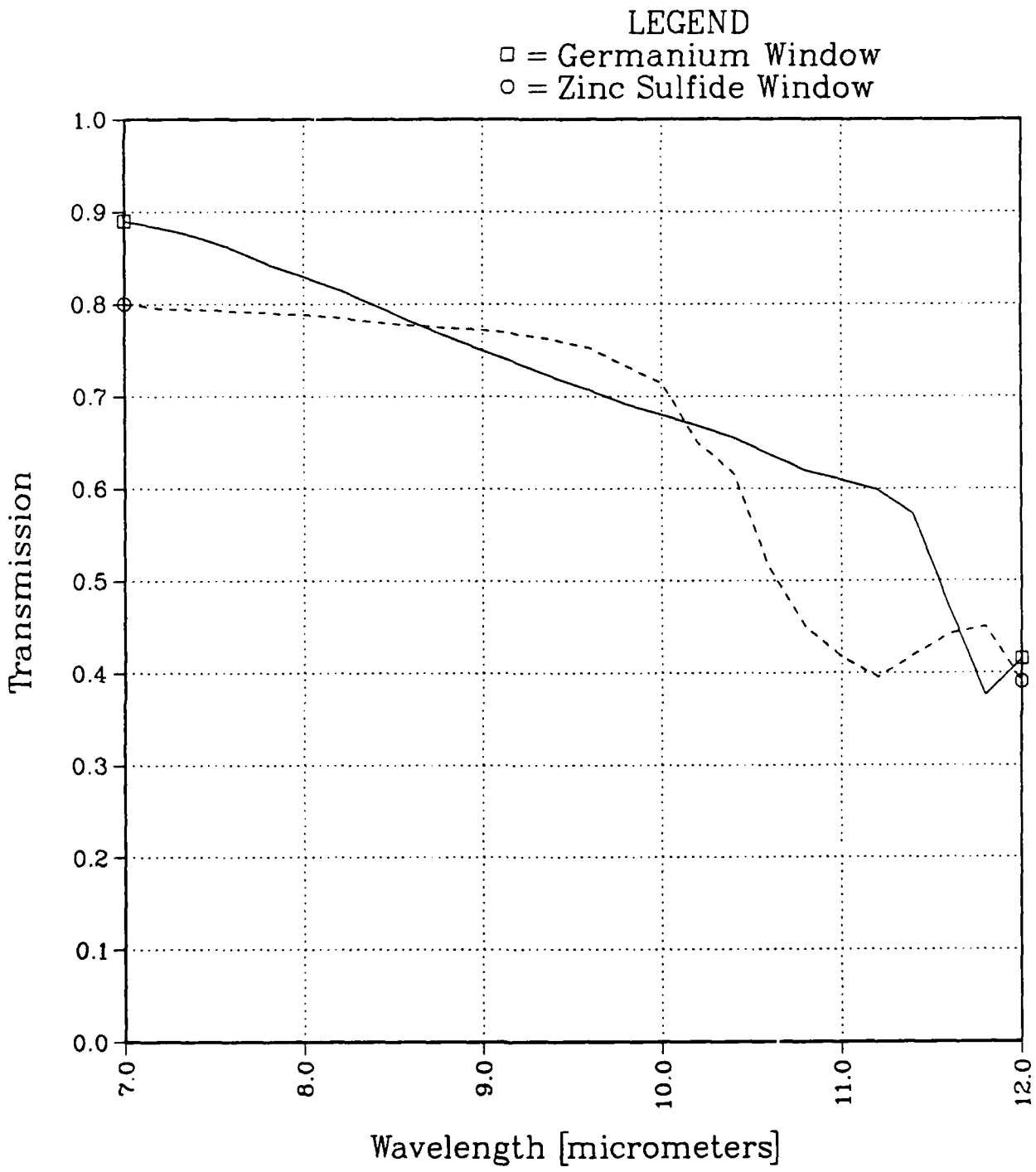

Figure 13. Aircraft Window Spectral Transmissivities

Table 1. In-Band Transmissivities of Aircraft Windows

Blackbody Temperature [Kelvin]	Germanium Window Transmissivity	Zinc Sulfide Window Transmissivity
220	0.676	0.624
240	0.682	0.632
260	0.687	0.639
280	0.691	0.646
300	0.694	0.651
400	0.708	0.669
500	0.715	0.679
1000	0.729	0.697
1500	0.732	0.701
2000	0.734	0.704

window, and so is slightly more desirable for mission purposes. Based on the values shown in Table 1, the germanium window is assumed to be the window of choice, and its properties will be used exclusively.

The in-band emissivity and reflectivity of the germanium window remain to be specified; unfortunately, no data on the spectral characteristics of these parameters is yet available. The only information that can be assumed is that the sum of the in-band transmissivity, emissivity, and reflectivity is approximately unity. (They would sum to exactly unity if the window were in thermodynamic equilibrium with its surroundings; however, the validity of such an assumption in the aircraft scenario is unclear.) As the in-band transmissivity has been calculated, both the emissivity and reflectivity may be bounded between zero and 'one minus the transmissivity.' Two limiting cases--zero reflectivity and zero emissivity--were therefore defined. Both of these were considered in the present study in order to bracket the range of possible window radiance levels .

For the purposes of this study, it was deemed acceptable to choose a single germanium window transmissivity value from Table 1 for use in Equation 1. A value of 0.69 was selected for this purpose. It was chosed primarily for compatibility with the expected window/aircraft interior temperatures that would be emitted/reflected. As such, it slightly overestimates the amount of transmitted sky radiance, and slightly underestimates the amount of transmitted plume radiance. Nevertheless, the amount of error should be insignificant to the study results. The choice of 0.69 transmissivity implies that the two limiting cases for the germanium window properties may also be expressed as "window emissivity = 0.31" and "window reflectivity = 0.31."

The only remaining parameters in Equation 1 that have not been explicitly defined are the physical temperatures of the germanium window, the FLIR telescope, and the aircraft interior. By assumption, the latter two were taken to be equal. Based on measured data, a range of temperatures was defined for both the window and the aircraft. The window temperature was assumed to lie in the range -35 to -10 degrees Celsius, while the aircraft interior/telescope temperature was assumed to be in the range +5 to +20 degrees Celsius.

2.2 SENSOR REQUIREMENTS FOR PLUME SENSING

With all of the quantities required by Equation 1 defined, it is possible to translate the predicted plume spectral radiances into corresponding in-band radiances at the CD-FLIR reference plane. The specific quantities to be defined for each of the three plume cases are as follows:

1. Minimum Radiance (L min): The minimum reference plane radiance that must be measurable; i.e., produce an output digital value above zero counts. This is defined as the sum

of the radiance contributions from the atmosphere, the aircraft window and the FLIR telescope.

2. Maximum Radiance (L max): The maximum reference plane radiance that must be measurable; i.e., produce an output digital value below 1023 counts. This is defined as the reference plane radiance equivalent of the brightest contour on the plume plus the radiance contributions from the atmosphere, the aircraft window, and the FLIR telescope.

3. Minimum Radiance Difference (dL): The minimum radiance difference to be resolved--both radiometrically and spatially--at the FLIR reference plane. This quantity is corresponds to the signal difference between the faintest plume radiance contours (translated to reference plane values). There is the additional requirement, however, that the contours must be separated spatially by a distance greater than the projected FLIR instantaneous field of view (IFOV). Table 2, below, shows the linear dimensions of the IFOV and the Total Field of View (TFOV) at the ranges appropriate to each of the three plume cases.

4. Plume "Dynamic Range" (PDR): A unitless quantity defined as: PDR = (L_max - L_min) / dL, it specifies how much dynamic range a sensor would need if had the radiometric sensitivity required to resolve 'dL' radiance differences.

5. Effective Plume Dynamic Range (EPDR): Analogous to PDR, except that EPDR = (L_max - L_min) / NER, where "NER" is the CD-FLIR's Noise Equivalent Radiance @ the reference plane. EPDR indicates how much system dynamic range (including the data recorder) is required to measure the entire plume signal, given the FLIR's existing radiometric sensitivity.

Table 2. View Geometries and CD-FLIR TFOV/IFOV for Plume Cases

	Case #1	Case #2	Case #3
Signature Type:	Weak	Intermediate	Strong
Range-to-Target:	140 km	110 km	170 km
Elevation Angle:	47 deg.	32 deg.	46 deg.
IFOV @ Range:	28 m	22 m	34 m
TFOV @ Range:	7.7 km	6.0 km	9.3 km

(Note: Nominal CD-FLIR IFOV = 200 urad; TFOV = 3.1 degrees)

As discussed in Section 2.1, limiting values were defined for several quantities such as the aircraft window emissivity and temperature. These ranges were combined to define a "Minimum Background" case and a "Maximum Background" case, as follows:

Minimum Background Case: This case represents the minimum possible radiance received from the germanium window and FLIR telescope, and corresponds to the following parameter values:

- Germanium window emissivity = 0.31
- Germanium window reflectivity = 0.
- Germanium window temperature = -35 deg. C
- CD-FLIR telescope temperature = + 5 deg. C

Maximum Background Case: This case represents the maximum possible radiance received from the germanium window and FLIR telescope, and corresponds to the following parameter values:

- Germanium window emissivity = 0.
- Germanium window reflectivity = 0.31
- Aircraft interior temperature = +20 deg. C
- CD-FLIR telescope temperature = +20 deg. C

Tables 3 and 4 show, for the Minimum and Maximum Background cases, respectively, the values of L_min, L_max, dL, PDR, and EPDR for each of the three plume signature cases. All radiance values are expressed as milliwatts/(cm**2-sr), which is a convenient unit for reference plane values. Listed at the bottom of the tables are the fractional contributions of the atmospheric path, aircraft window, and FLIR telescope radiances to the total background radiance, L_min. As shown, the total received background is dominated by the contribution of the telescope in the Minimum Background scenario (Table 3), and by the window reflection in the Maximum Background scenario (Table 4).

2.3 CD-FLIR CHARACTERISTICS VERSUS VGVFF GAIN SETTINGS

In this section, the performance of the CD-FLIR is predicted for each of the fifteen gain levels available with the VGVFF. The characterization is in terms of quantities that are directly comparable to those appearing in Tables 3 and 4. Specifically, for each VGVFF gain level, the following parameters are evaluated:

1. Minimum Measurable Radiance (L 0): For each gain setting, the reference plane radiance that corresponds to an output digital value of exactly zero counts.

2. Maximum Measurable Radiance (L 1023): For each gain setting, the reference plane radiance that corresponds to an output digital value of exactly 1023 counts.

3. Effective Noise Equivalent Radiance (NER eff): For each gain setting, the effective limit of radiometric sensitivity.

Table 3. Plume Measurement Requirements - Minimum Background Scenario

	Case #1	Case #2	Case #3
Signature Type:	Weak	Intermediate	Strong
L_min:[1,2]	0.758	0.764	0.758
L_max:	0.824	1.284	1.795
dL:	0.00052	0.00026	0.0041
PDR:	127	2000	250
EPDR:[3]	25	200	400
% of L_min due to			
Atmosphere:	4 %	5 %	4 %
A/C Window:	33 %	32 %	33 %
FLIR Telescope:	63 %	63 %	63 %

Notes:

1. See Section 2.1 for symbol definitions
2. All radiances in [mW/(cm**2-sr)] at FLIR internal reference plane
3. CD-FLIR Noise Equivalent Radiance = 0.0026 mW/(cm**2-sr) @ reference plane

Table 4. Plume Measurement Requirements - Maximum Background Scenario

	Case #1	Case #2	Case #3
Signature Type:	Weak	Intermediate	Strong
L_min:[1,2]	1.446	1.452	1.446
L_max:	1.512	1.972	2.490
dL:	0.00052	0.00026	0.0041
PDR:	127	2000	250
EPDR:[3]	25	200	400
% of L_min due to			
Atmosphere:	2 %	2 %	2 %
A/C Window:	54 %	54 %	54 %
FLIR Telescope:	44 %	44 %	44 %

Notes:

1. See Section 2.1 for symbol definitions
2. All radiances in [mW/(cm**2-sr)] at FLIR internal reference plane
3. CD-FLIR Noise Equivalent Radiance = 0.0026 mW/(cm**2-sr) @ reference plane

At the higher gain levels, this limit is set by the system NER value, which at the reference plane has a value of 2.6E-6 Watts/(cm**2-sr). At the lower gain levels, however, the radiance difference corresponding to one digital count may exceed this NER value. At these gains, the quantization grain is considered to be the limiting factor, and NER_eff is set equal to the radiance difference corresponding to one digital count.

4. Radiance Dynamic Range (RDR): For each gain setting, this is defined as RDR = (L_1023 - L_0) / NER_eff. For the lower gain settings where NER_eff is defined by quantization grain, RDR = 1023. For higher gains where there is more than one digital count on the rms noise level (i.e., the NER), RDR has a smaller value.

In order to define the above quantities for the various VGVFF gain levels, the following approach was used. Equation 2 (cf., Figure 5) was used to define L_0 and L_1023 by solving for the reference plane radiance that produces output digital values of zero and 1023, respectively. In order to invert Equation 2, values had to be defined for the reference plane responsivity (RRP(g)), the dc restoration radiance (L_clamp), and the digital dc bias level (D_clamp). A value of 435 counts, corresponding to the 3.4 volt dc restoration voltage, was used for D_clamp.

Because one of the primary issues of interest is the ability to measure cold sky backgrounds, the value of L_clamp was chosen to be its minimum possible value, as this permits the lowest value of L_0. Based on practical considerations, this minimum was defined to be the radiance corresponding to zero degrees Celcius. At lower clamp reference temperatures, it was assumed that frosting would occur, and the resulting apparent source temperature would remain near the freezing point.

The values of RRP(g) were defined by scaling the measured value at VGVFF gain 16 (i.e., the present HIGH gain setting) by the VGVFF gain factors shown in Figure 4. The laboratory measured value is RRP(g=16) = 1450. digital counts per mW/(cm**2-sr). Similarly, measured results at gain 16 were used to define NER_eff for the other gain levels. Laboratory measurements have shown that, at gain 16, the rms noise level corresponds to four digital counts. This value was scaled by the VGVFF gain factors to define the number of counts on the rms noise at other gain levels. For those gains where the rms noise level remained above one count, NER_eff was set equal to the system NER. When the noise level dropped below one count, the quantization grain was assumed to dominate. In those instances, NER_eff was set equal to the reciprocal of RRP(g), which gives the radiance difference corresponding to one digital count. Values of RDR, the radiance dynamic range, were then calcuated from the values of L_1023, L_0, and NER_eff.

The results of these calculations for the fifteen VGVFF gain

settings appear in Table 5. The values shown may be compared to the measurement requirements shown in Tables 3 and 4 to assess the utility of each gain setting. In particular, the following criteria may be defined for identifying the optimum gain settings:

1. L_0 vs. L_min: In order for the FLIR to collect useful data on a plume, it must be able to measure the background level. Thus, the value of L_0, the minimum measureable radiance, must be less than the background radiance, L_min. The most stressing requirement is from the Minimum Background Scenario (Table 3), plumes cases 1 and 3, in which L_min = 0.758 mW/(cm**2-sr). Table 5 shows that the VGVFF gain must be at setting 7 or lower to measure this.

2. L_1023 vs. L_max: In order to measure the brightest plume contour, L_1023 must be greater than or equal to L_max. The most stressing requirement occurs for the Maximum Background Scenario, plume case #3, where L_max = 2.490 mW/(cm**2-sr). Table 5 shows that all the VGVFF gain settings are capable of measuring this level.

3. NER_eff vs. dL: In order to measure the faintest contours of a plume, the FLIR's effective sensitivity, NER_eff, must be less than minimum plume signal difference, dL. This condition cannot be met for either plume cases #1 or #2, for which the values of dL are 0.00052 and 0.00026 mW/(cm**2-sr), respectively. These values are substantially smaller than the FLIR's Noise Equivalent Radiance of 0.0026 mW/(cm**2), which is the NER_eff available at gain settings 10 and higher. The plume case #3 requirement, dL=0.0041, can be met with gain gain settings 6 and higher.

4. RDR vs. EPDR: In order to measure the full signal range of a plume, the FLIR's radiance dynamic range, RDR, setting must be larger than the EPDR values of Tables 3 and 4. Plume case #3, with an EPDR value of 400, represents the most stressing requirement. Table 5 shows that gains 14 and lower have sufficient RDR to meet this requirement.

Overall, the above considerations show that gains 6 and 7 are the only ones that meet all the measurement requirements, given that the 'dL' requirements of plume cases #1 and #2 cannot be met with any gain. A choice of gain 6 or 7, however, results in reduced radiometric sensitivity compared to what the FLIR is capable of. The CD-FLIR's sensitivity limit is already very close to exceeding the SDIO specification. (Indeed, due to the 0.69 transmission of the aircraft window, the effective NESR outside the aircraft will approach 1.3E-6 Watts/(cm**2-sr-um).) One can therefore not afford to select a gain setting that does not allow the full system potential to be realized. Full system sensitivity is available at gains 10 and higher; however, these gains are unable to measure the very low background radiances associated with the plume sensing mission. The next section discusses how changing the dc restoration bias voltage can be used to solve this dilemma.

Table 5. Performance Characteristics of VGVFF Gain Settings

VGVFF Gain	L_0 [1-3]	L_1023 [1-3]	NER_eff [1,2]	RDR [1]
16	1.865	2.571	0.0026	256
15	1.766	2.704	0.0026	341
14	1.643	2.871	0.0026	445
13	1.497	3.068	0.0026	568
12	1.364	3.248	0.0026	682
11	1.223	3.438	0.0026	787
10	1.075	3.639	0.0026	930
9	0.967	3.785	0.0028	1023
8	0.831	3.969	0.0031	1023
7	0.665	4.193	0.0034	1023
6	0.389	4.565	0.0041	1023
5	~0.	5.120	0.0050	1023
4	< 0.	5.983	0.0065	1023
3	< 0.	7.148	0.0085	1023
2	< 0.	8.653	0.0110	1023

Notes:

1. See Section 2.3 for symbol definitions
2. All radiances in [mW/(cm**2-sr)] at FLIR internal reference plane
3. Assumes 0 °C dc restoration source; L_clamp = 2 165 mW/(cm**2-sr)

2.4 MODIFICATION OF THE DC RESTORATION BIAS VOLTAGE

Referring to Equation 2 (Figure 5), the digital value produced by any reference plane radiance level is determined by: (1) the radiance level itself; (2) the dc restoration source radiance; (3) the system responsivity, which is a function of gain setting; and (4) the dc restoration bias voltage. The previous section examined the effects of varying system responsivity by changing the VGVFF gain. The dc restoration source radiance is also adjustable, but has a practical lower limit due to condensation effects. This leaves the reference plane radiance and the dc restoration voltage as the parameters that might be adjusted to allow measurement of the cold sky background.

Initially, the reference plane radiance may not appear to be a free parameter, as the target and background to be viewed are not subject to control. As Tables 3 and 4 show, however, the total background level received at the CD-FLIR reference plane is strongly influenced by the temperatures of the aircraft window and internal environment/FLIR telescope. These temperatures are, in principle, subject to some amount of control. Thus, one approach to permit data collection at, for example, VGVFF gain 10 might be to heat the FLIR telescope in order to increase its radiant emission. For those used to dealing with dc coupled radiometers, especially background-limited ones, deliberately increasing the background radiance in this manner may seem complete folly. Nevertheless, for an ac coupled, non-background-limited sensor like the CD-FLIR, such an approach is completely viable.

An alternative to heating the telescope or the aircraft window is modification of the dc restoration bias voltage from its present value of 3.4 volts. Increasing this voltage level, which corresponds to increasing "D_clamp" in Equation 2 above its present nominal value of 435 counts, will lower the value of L_0 (as well as the value of L_1023) for any selected VGVFF gain. The amount by which L_0 and L_1023 are lowered for a given change in bias voltage depends on the gain setting.

Equation 2 may be used to calculate what value of D_clamp (and hence, what bias voltage level) is required to have L_0 equal to some desired level. This calculation was performed for several VGVFF gain levels to determine what bias voltage would be required to have L_0 equal to the 0.758 mW/(cm**2-sr) minimum background level from Table 3. The results appear in Table 6. Also shown are the modified values of L_1023 that would result from the new bias voltage. For comparison, Table 6 also shows the bias voltages required to have L_0 equal to the 1.446 mW/(cm**2-sr) Maximum Background radiance from Table 4. Values are only shown for those gains requiring a bias voltage higher than the present 3.4 volts.

The results shown in Table 6 may suggest that any of the VGVFF could be selected if the dc restoration bias were changed sufficiently. There are, however, several practical considerations that preclude setting the bias voltage to any arbitrary value. From the standpoint of radiometric calibration, the dc bias voltage

Table 6. DC Restoration Voltages Required for High Gain Operation Against Low Background Radiances

	Minimum Bkgd: L_min = 0.758 mW/(cm**2-sr)		Maximum Bkgd: L_min = 1.446 mW/(cm**2-sr)	
VGVFF Gain	V_clamp[1]	L_1023[2,3]	V_clamp	L_1023[2,3]
16	15.9	1.464	8.1	2.152
15	12.0	1.697	6.1	2.385
14	9.2	1.986	4.7	2.674
13	7.2	2.329	3.7	3.017
12	6.0	2.642	---	---
11	5.1	2.972	---	---
10	4.4	3.322	---	---
9	4.0	3.576	---	---
8	3.6	3.896	---	---

Notes:

1. V_clamp = dc restoration voltage [volts]
2. Radiances in [mW/(cm**2-sr)] at FLIR internal reference plane
3. Assumes 0 °C dc restoration source; L_clamp = 2.165 mW/(cm**2-sr)

should not be set higher than approximately six volts, which corresponds to a value of roughly 770 counts for D_clamp. The reason for this limit is as follows. The digital level of the left calibration source is always approximately equal to D_clamp, since the dc restoration source temperatures are slaved to the left reference temperature. Calibration of the FLIR's output is based on the two internal references. An adequate signal difference must be maintained between the two calibration references in order to permit responsivity determination. A left reference digital level of 770 counts permits up to 250 counts of separation between it and the right reference signal. This is an adequate amount for responsivity determination, but any smaller amount is not recommended. Note that the right reference signal must be higher than that of the left because the latter is assumed to be set at the lowest temperature achievable at the reference plane.

With the constraint that the dc bias voltage should be set no higher than about six volts, Table 6 shows that, for the minimum background condition, VGVFF gains 13 and higher cannot be used against the Minimum Background scenario. Referring back to Table 5, gains 9 and below result in less than full radiometric sensitivity. This leaves gains 10, 11 and 12 as the only remaining candidates. The performance differences between these gains are not great, and any of them might reasonably be selected. Gain 10 offers the most dynamic range, while gain 12 provides the best resolution of the system noise level. This latter consideration may prove to be important if analog recording is used with the CD-FLIR, since boosting the sensor noise level above that of the video electronics will be necessary to realize the full system sensitivity.

2.5 RECOMMENDED CD-FLIR HARDWARE MODIFICATIONS

Based on the results of Sections 2.3 and 2.4, a set of recommended hardware modifications may be formulated that will allow the CD-FLIR to collect full-sensitivity data against cold sky backgrounds. This set is presented below. The primary modifications involve selecting new VGVFF gains and adjusting the dc restoration bias voltage. In addition to these, several other modifications that may be necessary or desirable are described. The recommendations have been fomulated to minimize the extent and cost of the modification efforts. Based on conversations with Texas Instruments personnel familiar with the CD-FLIR, the modifications are all believed to be relatively minor.

Several options are presented under the recommendations for new VGVFF gain settings. These reflect the uncertainty surrounding: (1) the optical properties of the germanium aircraft window; and (2) whether digital or analog recording will be employed with the CD-FLIR. The Minimum and Maximum Background scenarios of Tables 3 and 4 represent a fairly wide range of background radiances. Depending on the degree to which the germanium window is emissive or reflective, the actual background level will fall somewhere within this range. Until the necessary

measurements are made to resolve this question, the "worst case" condition represented by the Minimum Background situation must be assumed, and VGVFF gains chosen accordingly. If, however, the actual background is closer to that of the Maximum case, another choice of VGVFF gains will provide the best performance. Gain recommendations for both of these possibilities are given.

The VGVFF gain options are also specified in terms of whether digital or analog recording will be used. The performance differences between digital and analog recording are discussed further in Section 3.0.

The recommended CD-FLIR hardware modifications consist of the following:

1. New VGVFF Gain Settings: Presently, VGVFF gain settings 2, 13, and 16 are connected to the gain selector on the FLIR control panel. It is recommended that gain 2 be retained for missions involving very hot targets (e.g., launches) as it permits the highest values of L_1023. One of the remaining two gains should be replaced by gain 6. This level will be used for: (1) plumes having signal levels equal to or larger than that of the strong signature case considered in this study; (2) other missions involving larger radiance levels than have been considered in this study, but not so large as to require the relatively insensitive gain 2. Depending on the expected background radiance levels and the data recording method to be used, the third gain setting--which will represent the full-sensitivity mode--should be chosen as follows:

- Digital recording, either Background: Gain 10
- Analog recording, Minimum Background: Gain 12
- Analog recording, Maximum Background: Gain 14

The reasons the above gains were selected are as follows: If digital recording is available, gain 10 is the obvious choice as it permits full sensitivity, affords the largest dynamic range, and--combined with the appropriate increase in the dc bias voltage--may be used against either the Minimum or Maximum Background scenarios. If analog recording is used, then the highest possible gain setting allowed by background radiance considerations should be chosen to permit maximum sensitivity.

2. New DC Restoration Bias Voltage: Depending on the expected background radiance levels and the data recording method, the present 3.4 volt bias voltage should be changed to the following:

- Digital recording, Minimum Background: 4.5 volts
- Digital recording, Maximum Background: no change
- Analog recording, Minimum Background: 6.1 volts
- Analog recording, Maximum Background: 4.8 volts

The above values correspond to the gain recommendations given above. An extra 0.1 volts has been added to the Table 6 values.

3. Store New Channel Normalizations: For any new gain levels selected, new channel normalization coefficients should be computed and stored in the system firmware. Recall that there is only room for normalization of two gain levels. It is recommended that the present practice of using VGVFF gain level 2 unnormalized be continued.

4. Add Display Readouts of Internal FLIR Temperatures: This recommendation applies primarily to the analog recording situation. The FLIR telescope and internal optics are instrumented with temperature sensors that provide information required for radiometric calibration. Presently, the readout from these sensors appears only in the image headers of the digital data stream. If analog recording is to be used, these values--particularly the telescope temperature--must be read out by some other means, either manually or automatically.

The above recommendations represent the minimum set necessary to make the CD-FLIR a useful ARGUS sensor. A number of additional modifications, most of which are more-extensive versions of those already identified, are mentioned below. While they represent somewhat greater modification effort, they would permit much greater flexibility in adjusting the FLIR's ten-bit dynamic range to a desired range of absolute radiances without compromising sensitivity. It is believed that the modifications suggested below could be implemented with a reasonable amount of effort, although this has not been verified with the sensor manufacturer.

5. Operator-Selectable DC Bias Voltage: Rather than make a "permanent" modification to the existing 3.4 volt dc restoration voltage, a switch could be added to the FLIR control panel that would allow an operator to select a desired bias voltage. The number of available voltages should probably be restricted to two or three discrete values, for example, 2.0 and 6.0 volts. This arrangement would permit full-sensitivity data collection against hot targets and cold backgrounds, respectively. One drawback of this scheme results from the dependence of the channel normalization coefficients upon the dc bias voltage. Thus, only two gain/bias voltage combinations could be normalized in firmware. This is primarily a cosmetic issue, however, as unnormalized data can be corrected off-line with appropriate processing.

6. Additional Operator-Selectable Gains: The present limit of three gain settings on the FLIR control panel could be removed. Conceivably, a thumb-wheel arrangement could permit access to all 15 VGVFF gain levels, thus affording maximum system flexibility (particularly if combined with the adjustable bias voltage option mentioned above).

As a final caveat, it should be understood that the performance predictions of Section 2.3--and consequently, the recommended modifications in this section--are based on laboratory performance measurements of a CD-FLIR unit that is not the one

being made available to the ARGUS program. The two units are supposed to be identical, but some small (or perhaps not so small) differences in performance between the two must be expected. An additional recommendation is therefore that the relevant performance parameters (e.g., responsivity, noise level, telescope transmission, etc.) be measured for the actual unit to be used on the ARGUS. Using these measured parameters, the analysis presented in Section 2.0 of this report should be repeated, and, if necessary, the specific recommendations of this section revised.

3.0

CD-FLIR PERFORMANCE WITH ANALOG VIDEO RECORDING

In Section 3.1, the effects of analog video recording upon system performance are identified and, to the extent possible, quantified. Section 3.2 addresses the specific issue of the impact of analog recording upon calibration accuracy.

3.1 ANALOG RECORDING EFFECTS

The performance of the CD-FLIR as measured at its analog video output is inferior in several respects compared to that obtained at the digital output. Three principal areas of performance degradation may be identified: (1) radiometric sensitivity; (2) spatial resolution; and (3) radiometric calibration accuracy. Item (3) is discussed in Section 3.2, while items (1) and (2) are addressed below.

3.1.1 Reduction in Radiometric Sensitivity

As noted in Section 1.1, the quoted NESR value for the CD-FLIR (i.e., 8.7E-7 Watts/(cm**2-sr-um)) pertains only to digital data. The effective NESR value at the analog output has not been measured by ERIM, but is expected to be 5-10 times larger than that of the digital output. This reduction reflects the smaller dynamic range (i.e., larger noise level) associated with the FLIR's analog circuitry. Additional degradation associated with the analog recording process may also be expected, depending on the quality of the recording equipment used.

3.1.2 Reduction in Spatial Resolution

Due to a number of effects, the CD-FLIR's spatial resolution performance is degraded in both the vertical and horizontal directions with analog output. Figure 7 illustrates the line-averaging scheme used to create 240 analog video field lines from 320 digital frame lines. This process alone results in a factor of two loss in vertical resolution (in addition to introducing the position-dependent, vertical spatial frequency response illustrated in Figure 8). In the horizontal direction, the effective bandwidth reduction associated with transforming 1024 samples into an RS-170 video line causes an effective resolution loss. The amount of loss has not been quantified by ERIM, but is expected to also be as large as a factor of two. These levels of resolution degradation are potentially serious as the nominal Instantaneous Field of View (IFOV) in the vertical direction is 200 microradians with digital output, while SDIO's resolution specification is 100 microradians. Thus, the FLIR's vertical resolution with analog recording may be over four times this value.

The line averaging used to create analog data produces another effect that further degrades spatial resolution in both directions

whenever there is relative motion between sensor and target. The effect is one of motion smearing, and results from the fact that any two digital lines averaged to create an analog line are generated from both directions of the CD-FLIR's bidirectional scan. Consequently, pixels that are vertically adjacent, but which were sampled at different points in time, are averaged to create each analog video line. For a fixed scene, the vertically adjacent pixels are also spatially contiguous, but this is not true if the scene moves significantly during the time between samples. Depending on the direction of scene motion, both the vertical and horizontal effective resolutions can be degraded by this effect. To further complicate matters, the time difference between vertically adjacent pixels varies linearly over the field of view. At the left edge of the FOV it is roughly 5 milliseconds, while at the right edge it is over 25 milliseconds. This represents a second way in which the resolution of the analog output can become spatially-varying.

3.2 RADIOMETRIC CALIBRATION ACCURACY WITH ANALOG RECORDING

In addition to the loss of fine spatial and radiometric detail, use of the CD-FLIR's analog output imposes limits on the achievable radiometric calibration accuracy. There are several causes of this effect. Most of these derive from the line averaging scheme discussed above, and are discussed further in Section 3.2.1. Section 3.2.2 then presents the results of an analysis in which simulated analog data was calibrated and the resulting radiometric errors quantified.

3.2.1 Analog Calibration Errors

Calibration errors in analog data can grouped into two general categories: (1) those which result from the creation of the analog data from the original digital data; and (2) those which result from the processing subsequently applied to the analog signals.

Addressing the latter category first: The CD-FLIR analog processing circuitry is capable of applying non-linear, scene-dependent signal transformations (i.e., histogram equalization functions) to the raw analog signals generated from the digital output. The purpose of these transformations is cosmetic, as they optimize the scene content in terms of the range of image greytones presented to an observer. In general, such transformations also destroy the radiometric meaning of the signal values, as the exact mapping function used, being scene-dependent, is not known.

Fortunately, the FLIR's histogram equalization function (which is known as the 'AUTO' mode on the FLIR control panel) may be disabled, in which case the output analog signal levels are linearly related to the raw values produced from the digital data. In this, the 'MANUAL' mode, the display mapping is controlled by operator-adjustable gain and offset (i.e., contrast and brightness) controls. Although they affect the signal levels in a linear manner, these controls could easily be mis-used to cause

calibration errors. As an example, calibration of analog data will probably require the collection of pure sky background images in order to define corrections for images containing plumes. If so, it will be necessary to ensure that the same gain and offset settings are used during the collection of both types of images. Failure to do so would produce potentially large calibration errors on the plume.

Apart from the calibration errors that may be introduced by analog signal processing, the averaging scheme used to create the analog video lines from the original video lines (cf., Figure 7) introduces inherently unavoidable errors. The primary effect results from the averaging together of signals exhibiting droop in opposite directions. This precludes the possibility of correcting the droop, which is a cornerstone of the existing digital data calibration methodology. Figure 14a shows actual digital data for both scan directions from a single detector channel that represent a moderately cold, uniform scene. Figure 14b shows the result of applying ERIM's droop-correction algorithm to this data. As shown, the algorithm removes the droop-induced signal errors from both scans. The constant offset between the corrected signals results from a temperature difference between the dc restoration sources used for the two scans. This offset difference vanishes when the pixel values are converted to absolute radiance. Section 3.2 defines the radiometric errors that would result from calibrating analog data created by averaging signals such as those shown in Figure 14a.

The digital-to-analog line generation scheme also averages together any non-uniformities of the two dc restoration radiance sources. If severe enough, non-uniformity on either source can result in cutoff or saturation of scene features within certain areas of the field of view. This effect, while highly undesirable, can at least be identified in the digital data by the presence of pixels having values of zero or 1023, respectively. In the analog data, however, cutoff or saturated values may be averaged with valid data (from the other scan) to produce a result that, while in error, appears to be valid.

In addition to correcting droop, the existing digital calibration methodology also corrects several other sensor-induced signal artifacts. In principle, a similar methodology could be defined for the FLIR's analog output. Such a scheme would still require digital image processing operations, however. Moreover, the required calibration-related data files (e.g., telescope transmission masks, internal vignetting masks, etc.) should still be created from digitally-recorded laboratory measurements. The inability to properly droop-correct the analog data limits its utility for accurately defining these correction functions.

3.2.2 Analysis of Droop-Induced Calibration Errors

A computer program was written to simulate the effects of calibrating CD-FLIR analog output data. The simulation was limited to completely uniform scenes as this simplification permits a

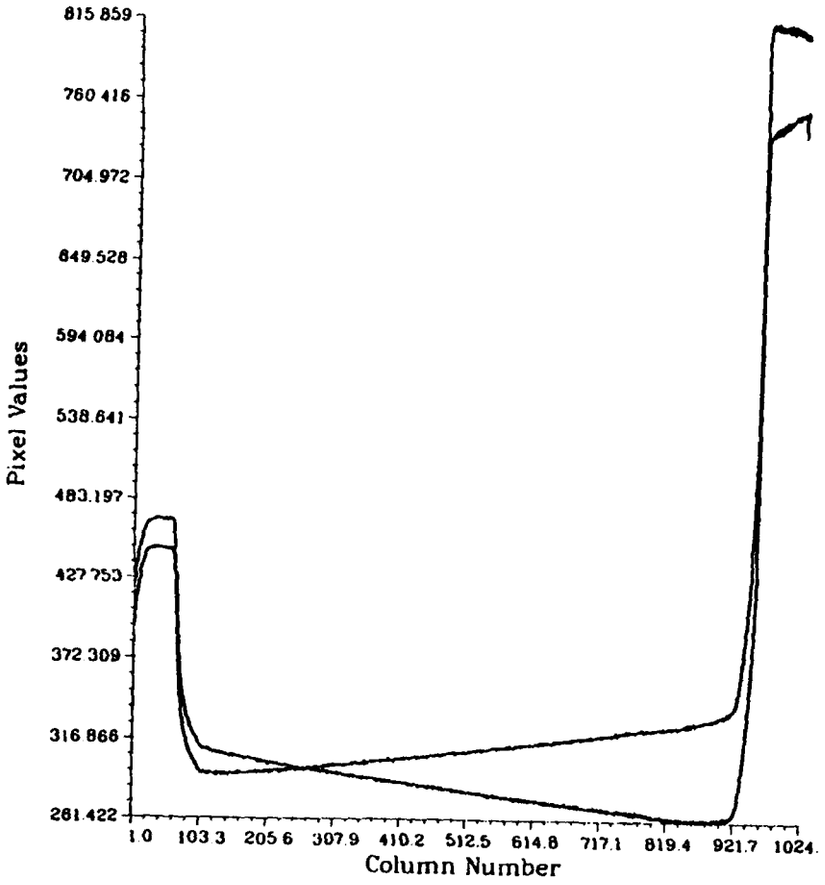

(a) Drooped Signal of Uniform Scene

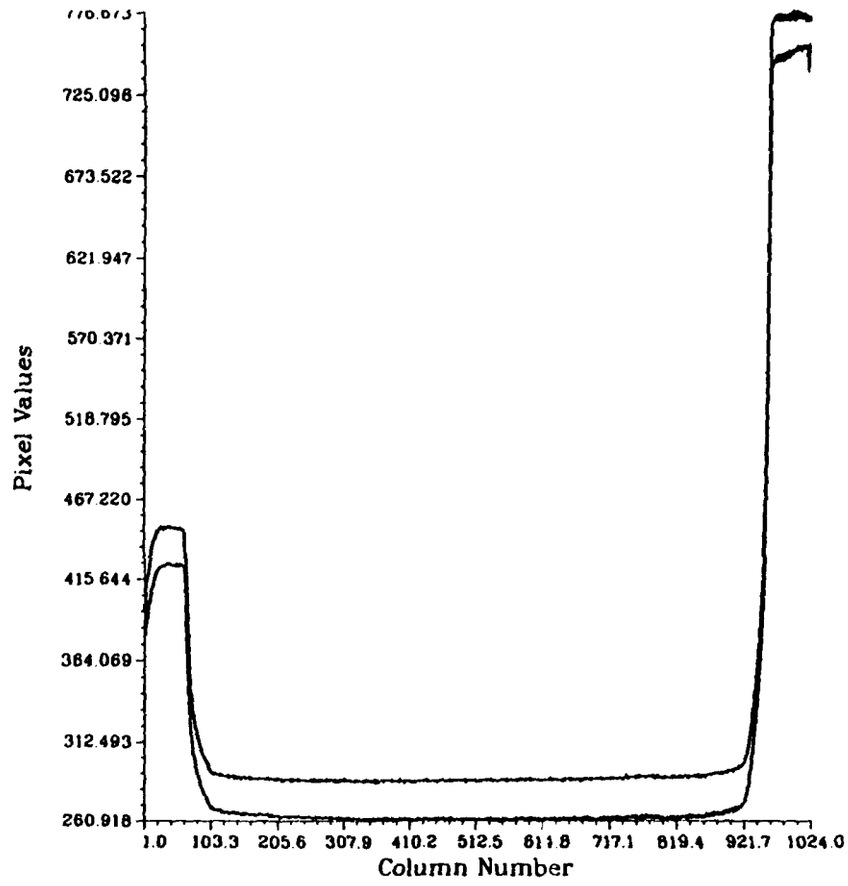

(b) Signal After ERIM Droop Correction Algorithm

Figure 14. Example of Drooped Digital Output Signal

analog signal levels. The expression itself is rather lengthy and is not presented here, but consists simply of a superposition of six decaying exponential responses, each appropriately weighted and delayed. Three of the six are contributed by each of the two scan directions. Within a scan, the three responses correspond to the uniform scene and the two calibration references.

Two basic scenarios were hypothesized, both involving cold scenes meant to represent a uniform sky background. The first, Scenario A, represents the existing dc restoration bias level of 435 counts (i.e., 3.4 volt bias voltage). The second, Scenario B, represents a bias level of 770 counts, which corresponds to a bias voltage of 6.0 volts, the upper limit discussed in Section 2.4. For each of these cases, a uniform reference plane radiance of 0.76 mW/(cm**2-sr) was assumed. This value was taken from the Minimum Background case shown in Table 3. The digital signal level corresponding to this scene radiance was chosen to be approximately 25 counts for both scenarios. The equivalent system responsivities implied by this condition are such that Scenario A corresponds to VGVFF gain 7, while Scenario B corresponds to gain 12. The right calibration reference digital value was chosen to be approximately 950 counts in both scenarios. The left reference value was set approximately equal to the clamp level value appropriate to each scenario.

In each of the two scenarios, signals were simulated to represent: (1) an analog line resulting from two digital lines produced by a single detector channel; and (2) an analog line resulting from digital lines produced by two different channels. The errors in radiance that would result from a straighforward calibration (i.e., one based solely on the apparent calibration reference source signals) of these results were then computed as a function of horizontal position.

Figure 15 shows the results for the Scenario A - Single Channel case. Figure 15a represents the analog video line across the horizontal field of view; however, the plot axes are labeled in terms of the original digital values and pixel column locations. The solid line on the plot shows the result of averaging together two droop-corrupted digital lines. The dashed line represents the "ideal" signal that would result if droop did not occur (or was corrected prior to the line averaging). As shown, the two oppositely-drooping signals tend to cancel each other, and produce what appears to be a nearly perfectly corrected result--at least at the scale shown in the figure. This explains why droop effects are not noticeable to the eye when viewing the FLIR's analog output. Compared to the ideal (dashed-line) signal, the analog signal is biased upward by a nearly constant amount. Some slight curvature is detectable across the field, but does not appear to be significant.

Figure 15b, which depicts the resulting radiance calibration errors in microwatts/(cm**2-sr), shows that the offset and curvature appearing in Figure 15a is actually significant after all. The average error of roughly +130 uW/(cm**2-sr) corresponds

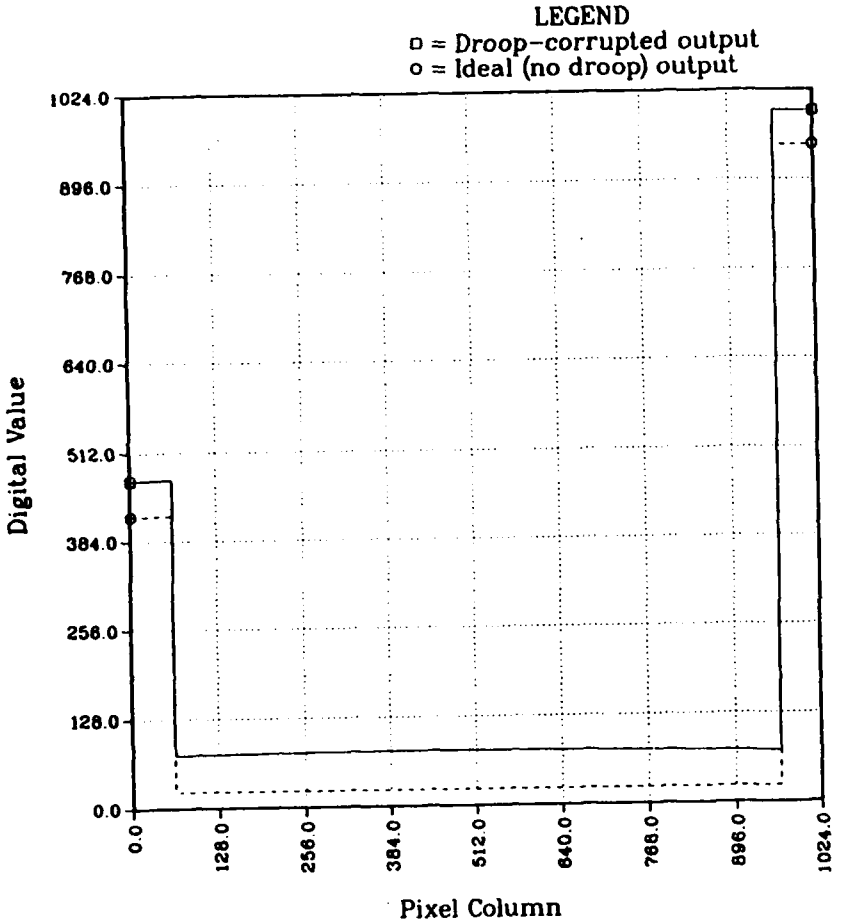

(a) Simulated Analog Signal Output

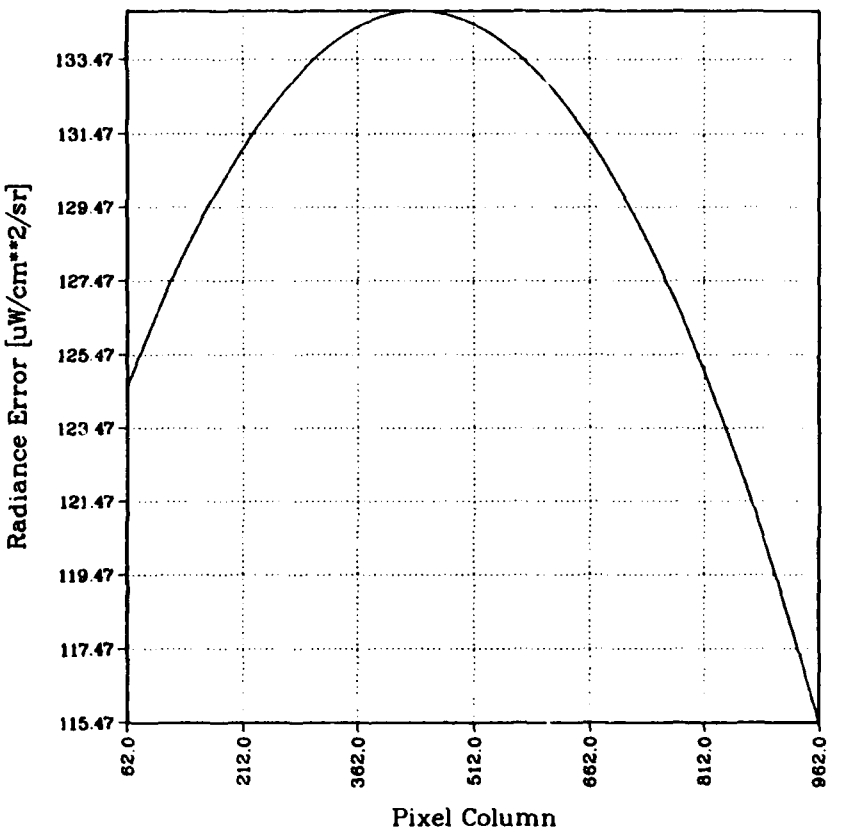

(b) Scene Radiance Calibration Error

Figure 15. Analog Data Simulation: Scenario A - Single Channel

to a +17 percent error in the determination of the 760 uW/(cm**2-sr) scene radiance. As shown, the amount of error varies in an asymmetric manner across the field of view.

Figure 16 shows the results obtained for the Scenario A - Two Channel case. The two channels were assumed to have a responsivity difference of 1 percent, an offset difference of 16 digital counts, and a difference in droop time constant of 9 percent. These values are representive of measured differences between CD-FLIR detector channels. The signal values shown in Figure 16a appear very similar to those of Figure 15a. The radiance errors in Figure 16b are, however, different from those of Figure 15b. The average error has increased to roughly +150 uW/(cm**2-sr), or nearly +20 percent of the absolute scene radiance. The spatial variation of the radiance error is also different from that of the previous case. Thus, each line of CD-FLIR analog data may have a unique error characteristic that depends upon the scene radiance level and the characteristics of the channel(s) that produced it.

Figures 17 and 18 show the Scenario B results obtained for the Single Channel and Two Channel cases, respectively. Compared to the Scenario A results, the analog signals shown in Figures 17a and 18a exhibit larger deviations from the ideal case. The differences are larger in terms of equivalent digital counts, but due to the higher system responsivity implicit in Scenario B, they do not correspond to significantly larger radiance differences. Indeed, the radiance error results shown in Figures 17b and 18b have smaller absolute values than their Scenario A counterparts. The range of error across the FOV is roughly the same in the two scenarios, that is, it is roughly 20 uW/(cm**2-sr) for both.

The absolute errors in Scenario B are smaller than those of Scenario A because the signal values of the scene are distorted less in relation to the calibration reference signals. This situation reflects the smaller asymmetry in the Scenario B signals that results from having the left and right calibration source signals more equally distant from the scene signal. In contrast, Scenario A has the left reference signal roughly 400 counts above the scene, while the right reference is over 900 counts above it. This larger asymmetry causes greater distortion of the scene signal relative to the references, and hence, larger absolute radiance errors. Somewhat paradoxically, therefore, having a large signal separation between the two calibration sources may seem desirable from the standpoint of responsivity determination, but actually induces larger calibration errors on a uniform scene if droop effects are not corrected.

The simulation analysis represented by Figures 15-18 has addressed the issue of analog calibration errors for uniform cold scenes. The real issue of interest involves the expected errors associated with calibrating analog imagery of missile plumes. This issue could also be investigated via signal simulations. The nature of the simulation would have to be numerical rather than analytical due to the complex spatial structure of the plume radiance field. This level of simulation could not be performed

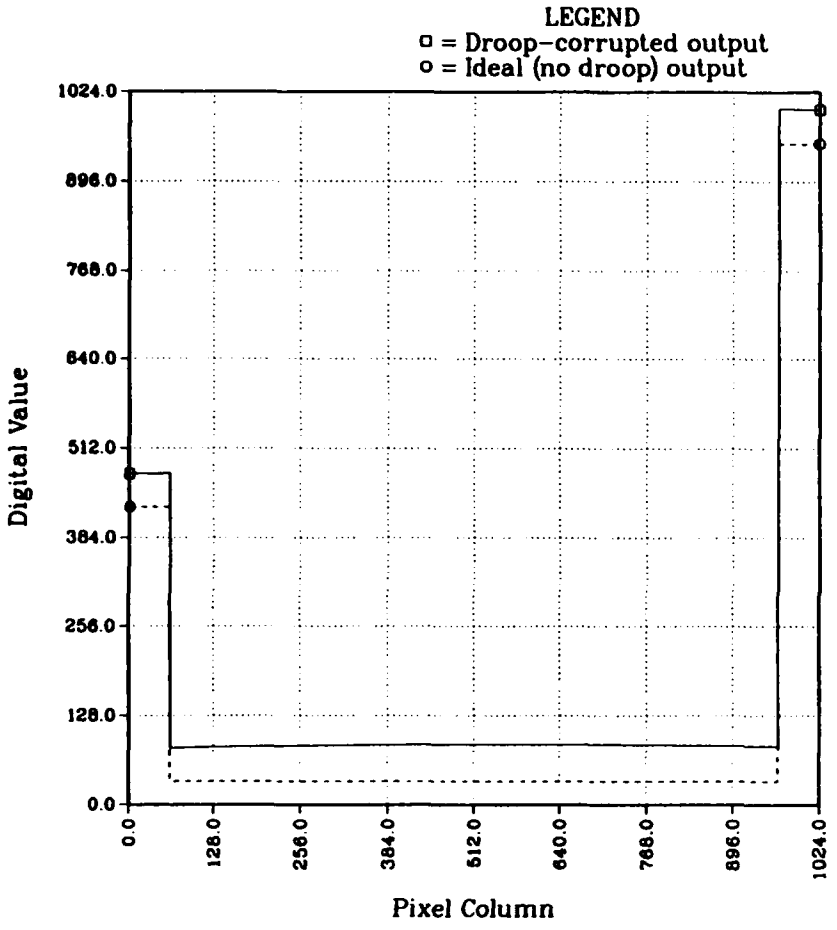

(a) Simulated Analog Signal Output

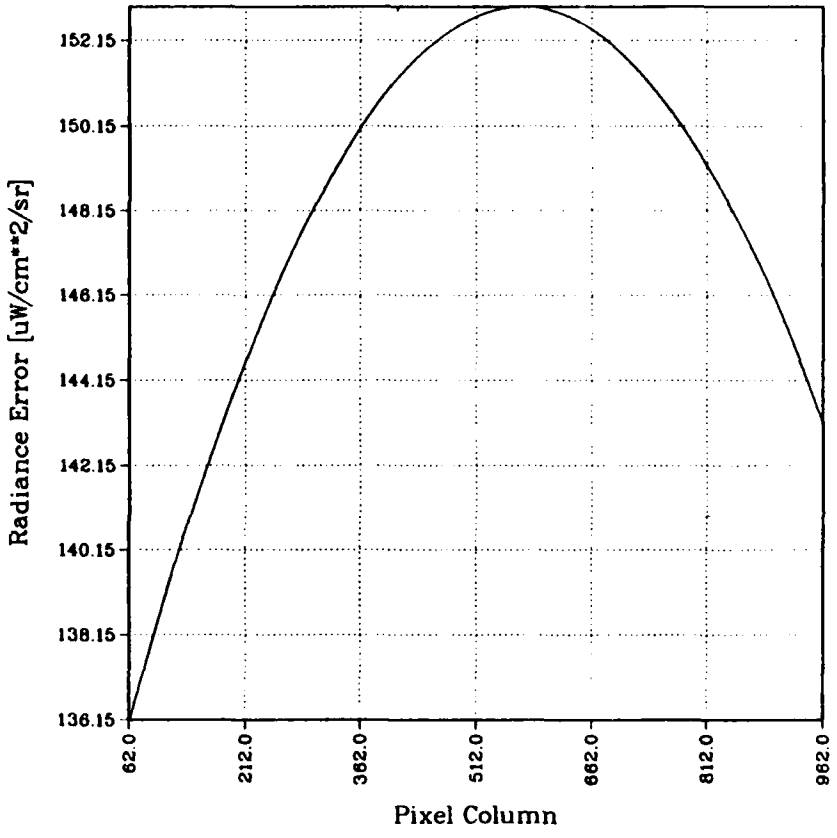

(b) Scene Radiance Calibration Error

Figure 16. Analog Data Simulation: Scenario A - Two Channels

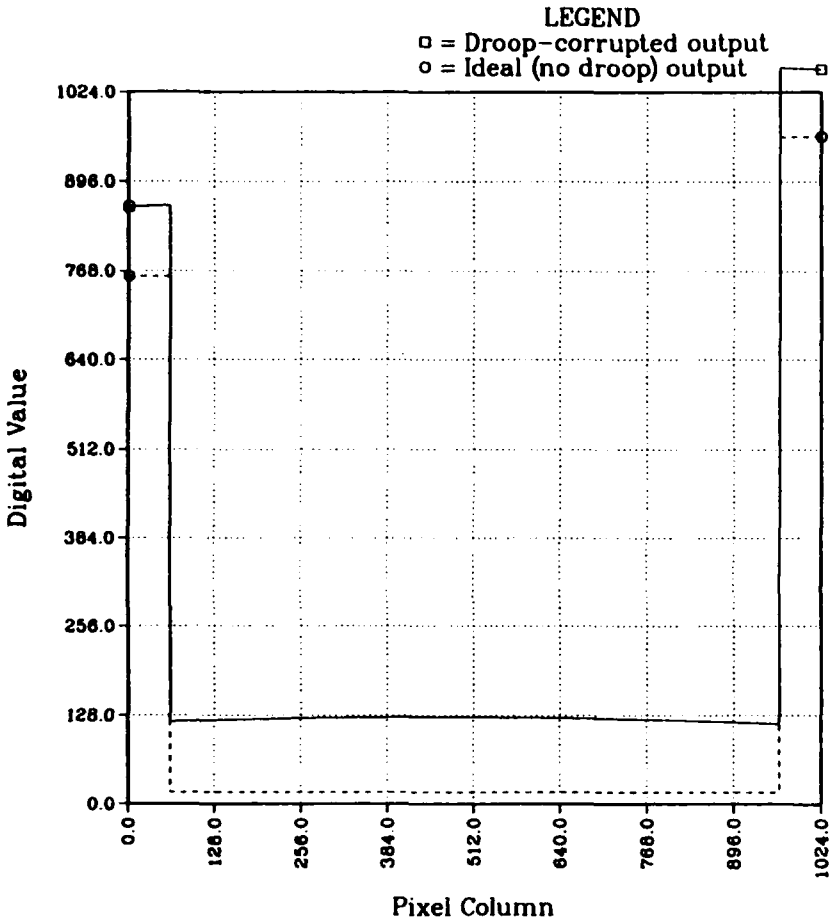

(a) Simulated Analog Signal Output

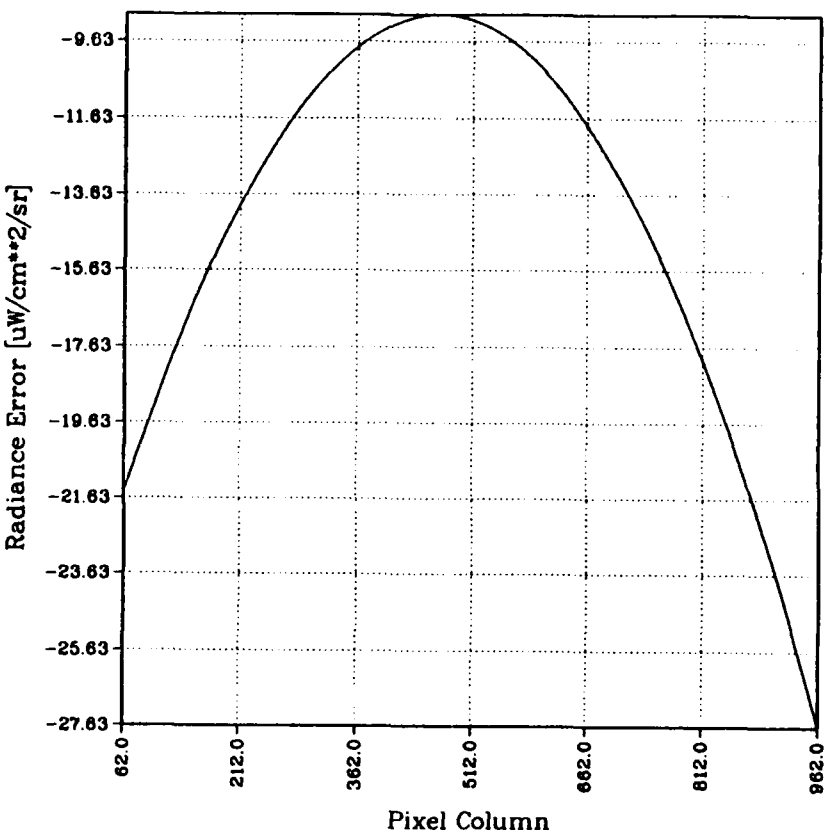

(b) Scene Radiance Calibration Error

Figure 17. Analog Data Simulation: Scenario B - Single Channel

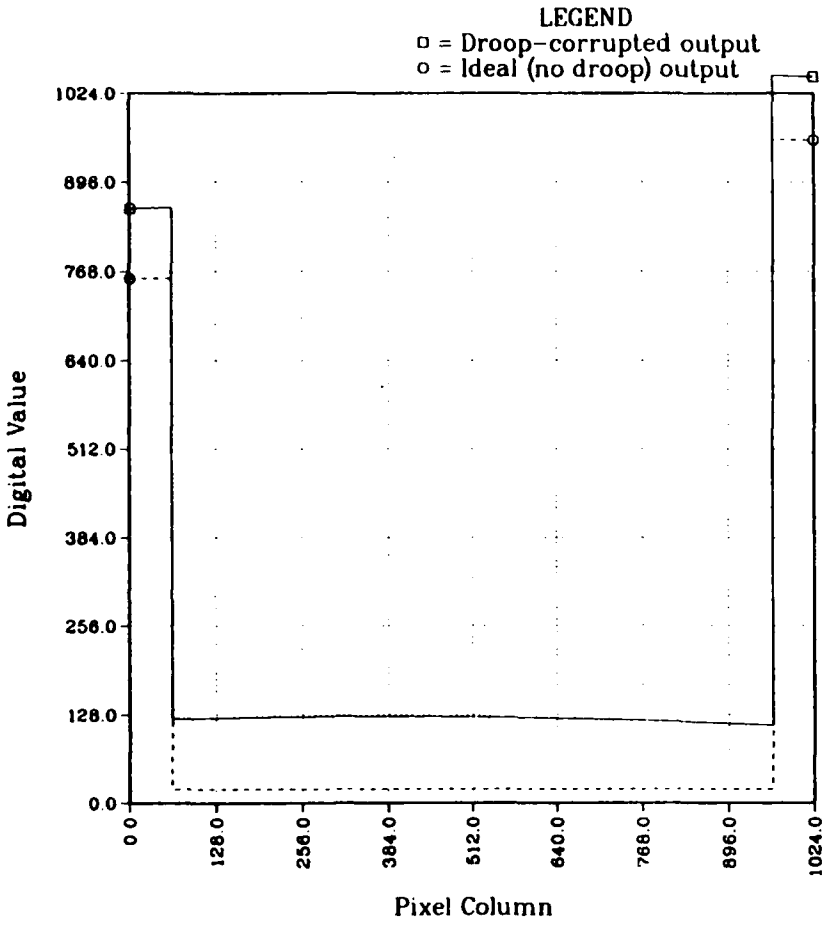

(a) Simulated Analog Signal Output

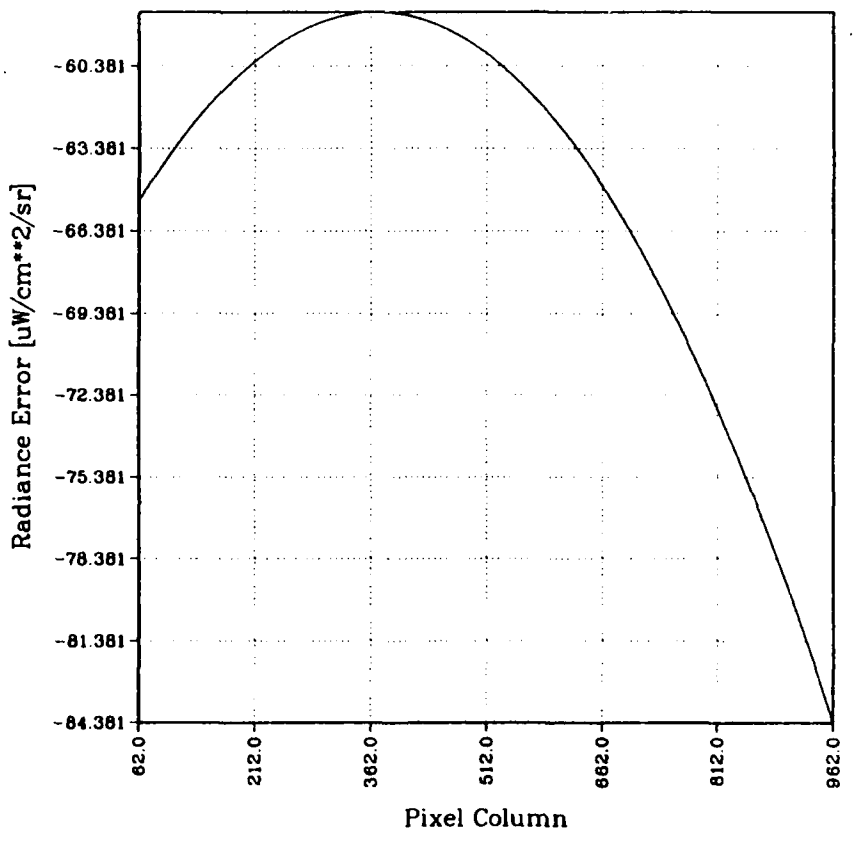

(b) Scene Radiance Calibration Error

Figure 18. Analog Data Simulation: Scenario B - Two Channels

within the scope of the present study. (Indeed, the simulation results presented above are the result of efforts outside the original scope of this study.) Some qualitative assessments are possible, however.

Recall that the plume signature predictions of Figures 9-11 do not include any background radiance contributions. Consequently, in order to validate the model predictions, one need only make accurate measurements of the difference between a plume signature and the total background. If it could be assumed that the plume-to-background signal differences were unaffected by droop, the absolute radiance errors on the background simulated in Figures 15-18 would become irrelevant. This assumption is valid to the extent that the spatial frequency spectrum of the plume signal has negligible low-frequency content. This occurs whenever the plume signal is spatially small and/or weak in intensity. This condition holds quite well for the weak signature plume of Figure 9. It holds somewhat less for the intermediate case, and lesser still for the strong signature case. Almost any plume signature will approximate the required condition, however, since the largest areas--i.e., those representing the lowest frequency components--are always those with the weakest signals. This statement is not quite true for those image lines containing the plume core, which by virtue of its intensity contributes significant low-frequency energy (i.e., produces a large average signal within the line). This effect, however, pertains to only a relatively small fraction of the total number of pixels on the plume. Overall, the situation is fortuitous in that the largest droop-induced, absolute radiance errors occur on the strongest signals. The weaker signals--for which a given absolute radiance error represents a larger percentage error--are comparatively unaffected.

The point of the preceeding argument is that the radiance errors associated with plume measurements may be much less than the errors predicted for uniform cold backgrounds. It is recommended, however, that this contention be explored further by performing the numerical simulation described above.

4.0

SUMMARY AND CONCLUSIONS

Three specific objectives were defined to assess the CD-FLIR's expected performance in the ARGUS environment:

1. Identify the hardware modifications necessary to permit data collection against very cold backgrounds with maximum radiometric sensitivity.

2. Assess the impact of processing data from the CD-FLIR's video output upon system performance and radiometric calibration accuracy.

3. Define the expected level of performance of the CD-FLIR in terms of its ability to measure missile plumes.

The conclusions and recommendations associated with each of these objectives are listed below.

4.1 HARDWARE MODIFICATIONS

The analysis presented in Section 2.0 resulted in the identification of several, relatively simple hardware modifications that should permit full sensitivity data collection against cold sky backgrounds and with enough dynamic range to permit measurement of the brightest plume contours. The recommended modifications primarily involve the selection of new gain settings already available with the FLIR, as well as adjusting the dc restoration bias voltage. The specfic modification recommendations are discussed in Section 2.5

4.2 IMPACT OF ANALOG DATA RECORDING

Section 3.0 identified the performance penalties associated with using the CD-FLIR's analog data output. The results may be summarized as follows:

Reduced Radiometric Sensitivity: With digital output, the CD-FLIR's NESR is 8.7E-7 W/(cm**2-sr-um) at the telescope aperture. The 0.69 effective transmissivity of the ARGUS aircraft window results in an effective value of 1.3E-6 at the window exterior. These values may be expected to increase an additional order of magnitude if analog recording is used.

Reduced Spatial Resolution: With digital output, the FLIR's IFOV has a nominal value of 200 microradians. With analog recording, this value will increase to at least 400 urad. In addition, the line-averaging scheme used to create analog video lines from digital image lines produces several effects (e.g., motion smear) that further degrade system resolution.

Radiometric Calibration Errors: An analysis was conducted to assess the level of droop-induced calibration errors in analog data. These errors result from the inability to correct droop in the digital data that is used to create analog output. Absolute radiance errors of the order of one hundred microwatts/(cm**2-sr) were found to apply to cold sky scenes. It is believed, however, that the radiance errors associated with plume signature measurement will be much smaller. Further study of this issue was not possible within the scope of this study, but is recommended as part of a future effort.

4.3 CD-FLIR PERFORMANCE AGAINST MISSILE PLUMES

The results of this study suggest that, with the appropriate hardware modifications, the CD-FLIR is capable of making useful plume signature measurements. The full range of plume signals should be measurable down to the spatial and radiometric resolution limits identified above. With digital recording, these limits approach very closely the performance specfications defined by SDIO. With analog recording, the performance penalties identified above are incurred.

4.4 SUMMARY OF STUDY RECOMMENDATIONS

The recommedations made in the previous sections are summarized below. Also included are recommendations for verifying the assumptions upon which the present study results are based.

It is recommended that:

1. Laboratory measurements should be made on the ARGUS CD-FLIR to quantify the sensor parameters critical to the present study results (e.g., responsivity vs. gain, noise levels, telescope transmission, etc.), but whose values are presently based upon measurements made on a different CD-FLIR unit. Ideally, the data from these measurements should be recorded using the existing CD-FLIR digital recording system.

2. The in-band emission and reflection characteristics of the ARGUS germanium window should be measured to define the total background radiance expected during ARGUS missions.

3. Based on the results of the above measurements, the gain analysis of Section 2.3 should be updated to revise the set of VGVFF gain settings recommended in Section 2.5.

4. After completing the above steps, the revised set of hardware modifications should be implemented on the sensor.

5. Due to the significant degradation of sensor performance associated with analog data recording, a suitable digital recording capability should be developed as soon as possible.

APPENDIX

INFORMATION ON PREDICTED PLUME SIGNATURES

INSTITUTE FOR DEFENSE ANALYSES
1801 N. Beauregard Street, Alexandria, Virginia 22311-1772 • Telephone (703) 845-2000

SCIENCE AND
TECHNOLOGY DIVISION

MEMORANDUM TO: Mr. Dave Witte, ERIM
FROM: Dr. William Jeffrey
SUBJECT: LWIR Predictions
DATE: 7 October 1989

Enclosed are predictions in the 8.0-12.0 micron band for three different systems using CHARM 1.2 (but with the particulate optical properties as provided in the upgraded CHARM 1.1). For all three systems I have included losses due to atmospheric absorption assuming the aircraft is at 12 km and the altitude of the target and range are as indicated on the contour maps. No other losses have been assumed for these calculations. The numbers on the contours refer to the log of the radiance in $W/cm^2/sr/um$, thus -5 indicates the 10^{-5} $W/cm^2/sr/um$ level.

The first system is a large liquid amine-fueled system flying at 114 km with a velocity of 3.6 km/s. The weak emission is due to the absence of any particulate matter in the plume. The second system is the Orbus I engine which will be used as the third and fourth stages for the upcoming Starbird demonstration flight. This system is rather small, but has a heavily aluminized solid propellant which accounts for the strong emission. The final case is the Antares which is a large system with an aluminized solid propellant.

I hope these estimates will be of use to you. If you require any additional information please do not hesitate to contact me.

cc: Maj. Dave Anhalt, SDIO/TNS

LIQUID BOOSTER RADIANCE (LOG W/cm2/sr/um) 8.0-12 um
ALT: 114 km, RANGE: 140 km, A/C: 12 km, 76 US STAND

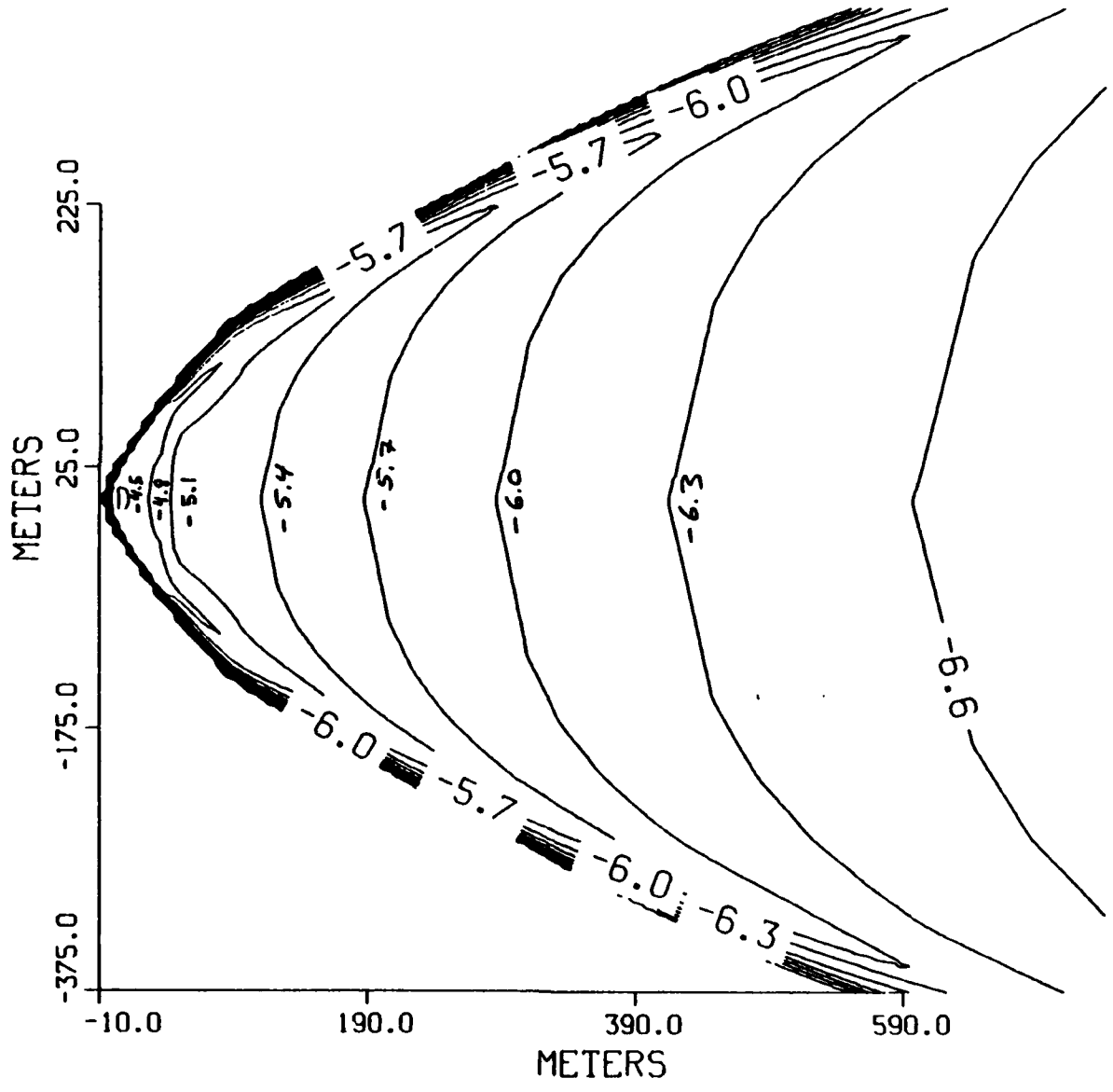

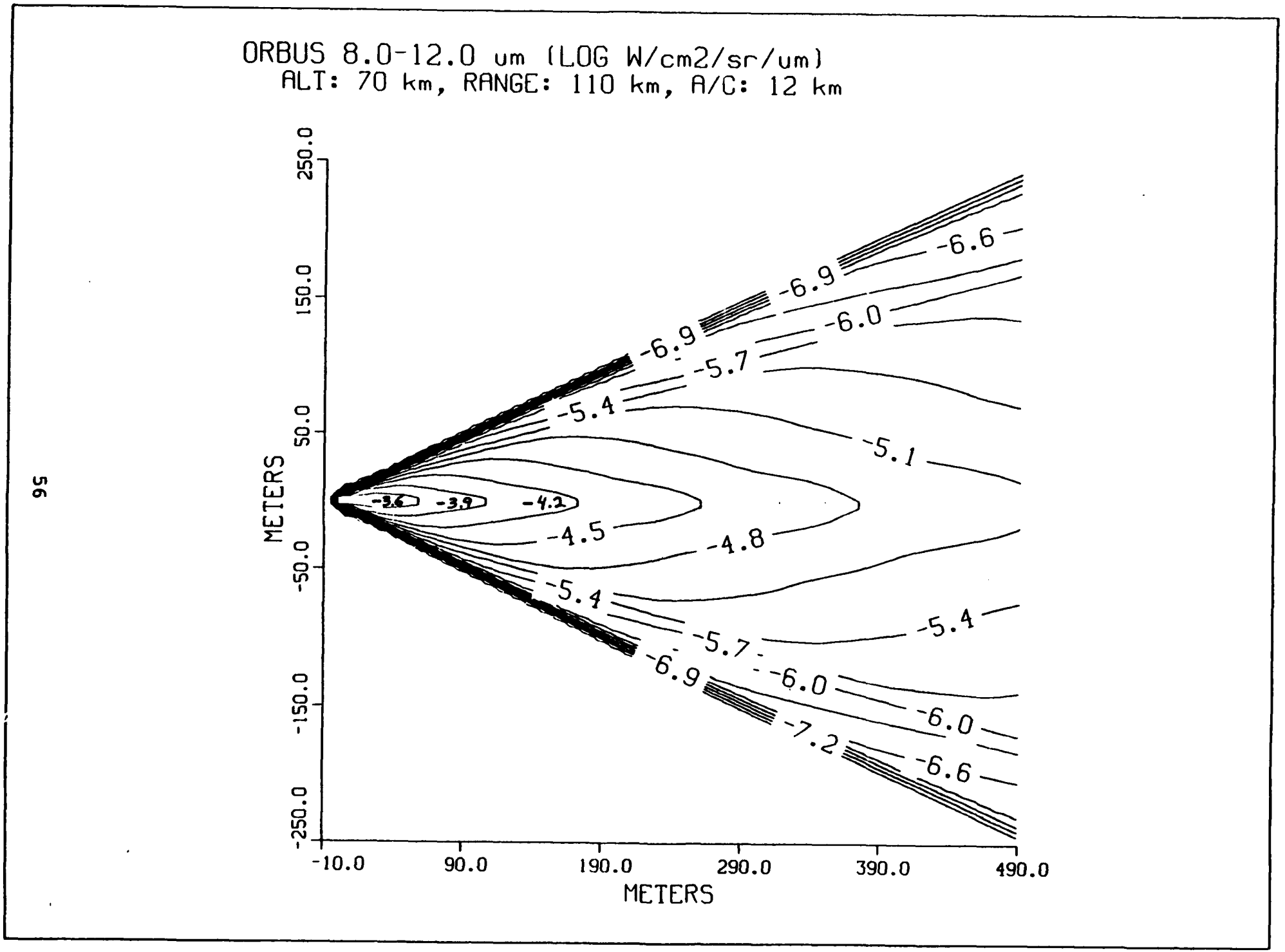
ORBUS 8.0-12.0 um (LOG W/cm2/sr/um)
ALT: 70 km, RANGE: 110 km, A/C: 12 km
250.0
150.0
50.0
-50.0
-150.0
-250.0
METERS
-10.0
90.0
190.0
290.0
390.0
490.0
METERS
-6.9
-6.6
-6.9
-6.0
-5.7
-5.4
-5.1
-3.6
-3.9
-4.2
-4.5
-4.8
-5.4
-5.4
-5.7
-6.0
-6.9
-6.0
-7.2
-6.6

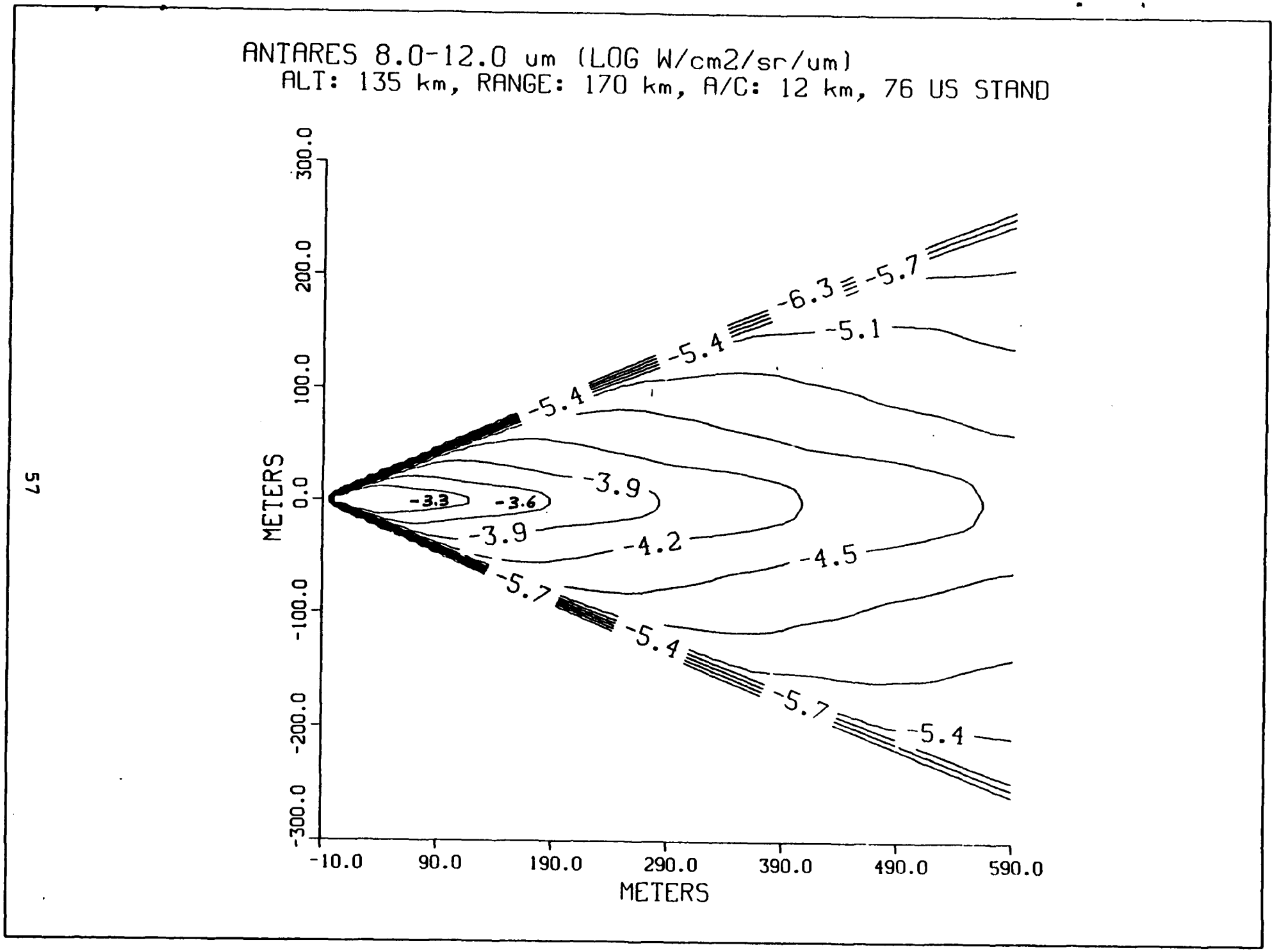
ANTARES 8.0-12.0 um (LOG W/cm2/sr/um)
ALT: 135 km, RANGE: 170 km, A/C: 12 km, 76 US STAND
300.0
200.0
100.0
0.0
-100.0
-200.0
-300.0
METERS
-10.0
90.0
190.0
290.0
390.0
490.0
590.0
METERS
-5.4
-6.3
-5.7
-5.4
-5.1
-3.9
-3.3
-3.6
-3.9
-4.2
-4.5
-5.7
-5.4
-5.7
-5.4